



Microneedles for non-transdermal drug delivery: design strategies and current applications

Jinhong Xu¹ · Xiangyi Liao² · Danli Chen² · Xiuzhuo Jia³ · Xufeng Niu²

Received: 7 December 2023 / Accepted: 8 October 2024
© Zhejiang University Press 2025

Abstract

Microneedles (MNs) are an innovative and viable option for drug delivery that offer the distinct advantages of minimal invasiveness, painlessness, stable drug loading, efficient drug permeation, and biocompatibility. MNs were first used to penetrate the skin surface and facilitate transcutaneous drug delivery with great success. Recent applications of MNs have extended to non-transdermal drug delivery, specifically, to various tissues and organs. This review captures the fabrication methods for MNs, discusses advanced design strategies for achieving controlled drug release, and summarizes current MN applications in delivering multiple therapeutic agents to the cardiovascular, digestive (e.g., oral cavity), reproductive, and central nervous systems. The findings in this review would contribute toward the improved designs of MN systems that can be modified according to purpose, including material selection, structural design, choice of fabrication methods, and tissue considerations, to determine the optimal therapeutic regimen for the target treatment area.

Jinhong Xu and Xiangyi Liao have contributed equally to this work.

✉ Xiuzhuo Jia
hestxrmyygrgk@163.com

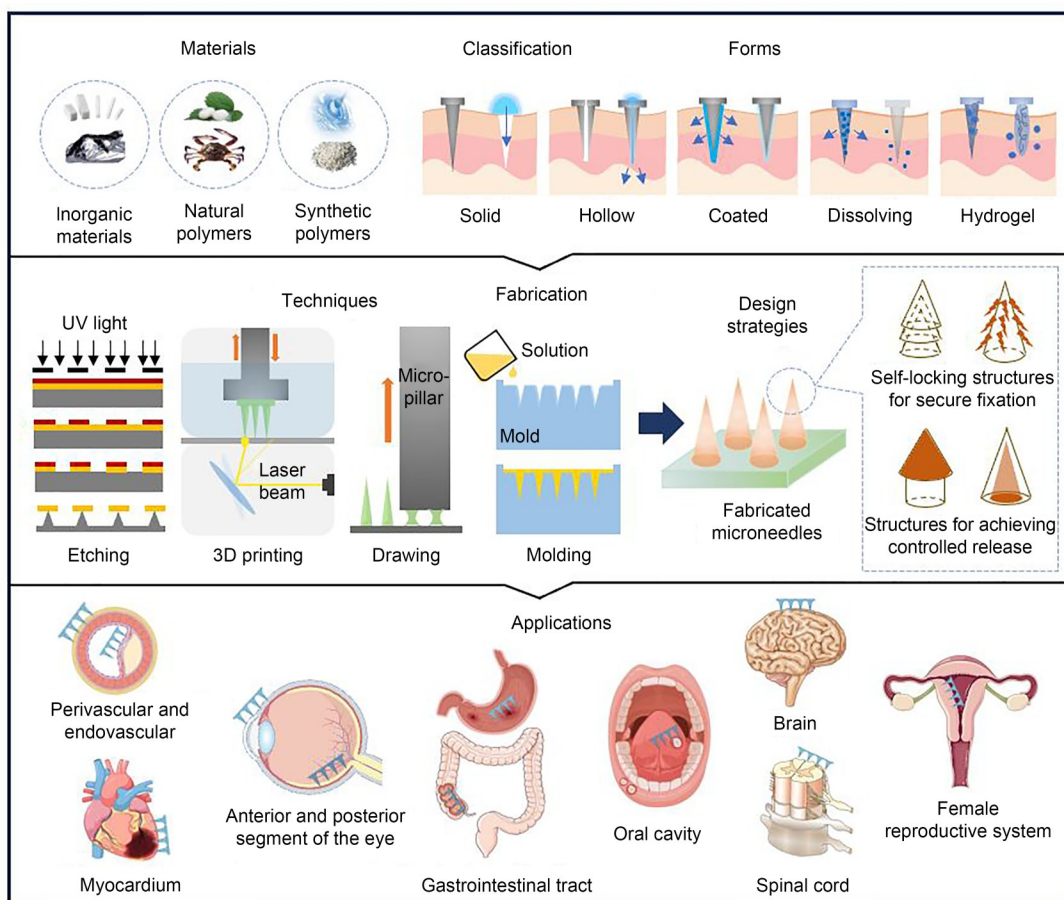
✉ Xufeng Niu
nxf@buaa.edu.cn

¹ Department of Pharmacy, The Fourth Central Hospital of Baoding City, Baoding 072350, China

² Key Laboratory of Biomechanics and Mechanobiology (Beihang University), Ministry of Education, Beijing Advanced Innovation Center for Biomedical Engineering, School of Biological Science and Medical Engineering, Beihang University, Beijing 100083, China

³ Department of Medical Business, The Fourth Central Hospital of Baoding City, Baoding 072350, China

Graphical abstract



Keywords Microneedles (MNs) · Biocompatible materials · Non-transdermal drug delivery · Controlled release

1 Introduction

Conventional transdermal drug delivery methods, including hypodermic, intradermal, and intravenous injections, can easily break through the stratum corneum with rigid needles and are cheap and convenient ways of drug delivery and body fluid collection [1]. Current methods of transdermal drug delivery can address drug efficacy decline after gastrointestinal (GI) action during oral administration and overcome poor drug permeation restriction during topical drug delivery; however, traditional needles can cause pain and tissue damage [2, 3]. Furthermore, a certain subpopulation of people are extremely afraid of needles and declare themselves as having blood–injury–injection (BII) phobia [4]. Microneedles (MNs) are micron-scaled needles that were initially used in the delivery of therapeutic agents through the skin. The concept was first proposed by Prausnitz [5] in 1998 to deal with all these questions raised on the use of

standard needles [5, 6]. As a third-generation enhancement strategy of transdermal drug delivery, MNs have become a major tool for macromolecule and vaccine delivery. Compared with other means of drug delivery mentioned above, current MN-based drug delivery systems have several advantages, including minimal invasiveness and a lower risk of infection. By physically penetrating the stratum corneum and increasing skin permeability, MNs provide an efficient method of transporting target drug molecules without stimulating the nerves, which can overcome the delivery efficiency issue with minimum tissue damage [7, 8].

With the development of materials science and microfabrication equipment upgrades, MNs consisting of an array of micron-scale needles can be manufactured into various forms. Typically, MNs can be sorted into four main categories: solid, coated, hollow, and biodegradable. Solid MNs are made of silicon and biocompatible metal, which can be coated or loaded with drugs. Hollow MNs have a chamber

inside and can be used for liquid drug infusion or body fluid sampling. Dissolvable MNs fabricated through biodegradable polymers can release drugs with the supporting hydrophilic material and rapidly dissolve into the interstitial fluid [9]. Hydrogel needles, a novel form of MNs, are currently being extensively explored. These MNs consist of crosslinked hydrogels loaded with drugs. Once they are applied onto the tissue surface and come into contact with an aqueous medium, these MNs swell to facilitate the influx of drugs into the tissues [10–12]. Various materials have been used in MN fabrication, including silicon, metals, ceramics, and natural and synthetic polymers. Different fabrication strategies have also been explored. For example, the needle can be shaped into pyramidal, conical, bullet-shaped, arrow-shaped, or other complicated geometry to perform specific applications [13, 14]. By piercing the skin barrier with the micron-scale needle array, macro- and micro-molecules can be delivered into the dermis of specific skin regions to perform various treatments, such as vaccine delivery, cancer therapy, hormone therapy, wound healing, and tissue regeneration (Fig. 1).

Over the past decades, although extensive developments of MN drug delivery still centered around transdermal implementations, ongoing investigations explored the utility of the technology in delivering drugs to other tissues and

organs, marking the preliminary exploration of non-transdermal drug delivery using MNs. More recent cutting-edge research has begun the exploratory application of MNs in these areas, and studies on expanding the structure and function of MNs are ongoing. In this review, we focus on the use of MNs in targeted delivery to soft tissues (Fig. 2). Applications for drug delivery into the scalp, nails, and bones are beyond the scope of this study because some of the design criteria differ from those for soft tissue, which either have extremely high mechanical requirements or lack the need for biodegradation. Furthermore, by discussing fabrication techniques, design strategy selection, and leading-edge achievements in MN development for the delivery of therapeutic drugs across different biological barriers, this review also provides a concise discussion of design principles of non-transdermal MNs for specific tissue applications. Overall, this review aims to minimize the gap between applied research and clinical translation while simultaneously proposing prospects for future research directions.

2 Advanced fabrication strategies and characterization of MNs

The combination of specific material selection and novel manufacturing technologies provides the premise for the

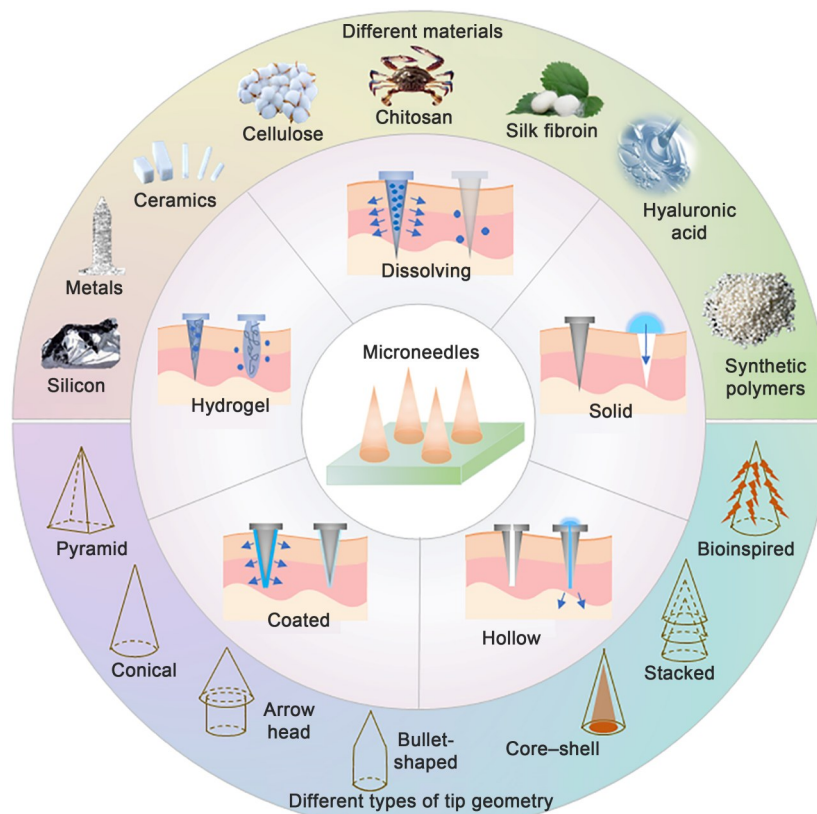


Fig. 1 Classification of microneedles under different criteria

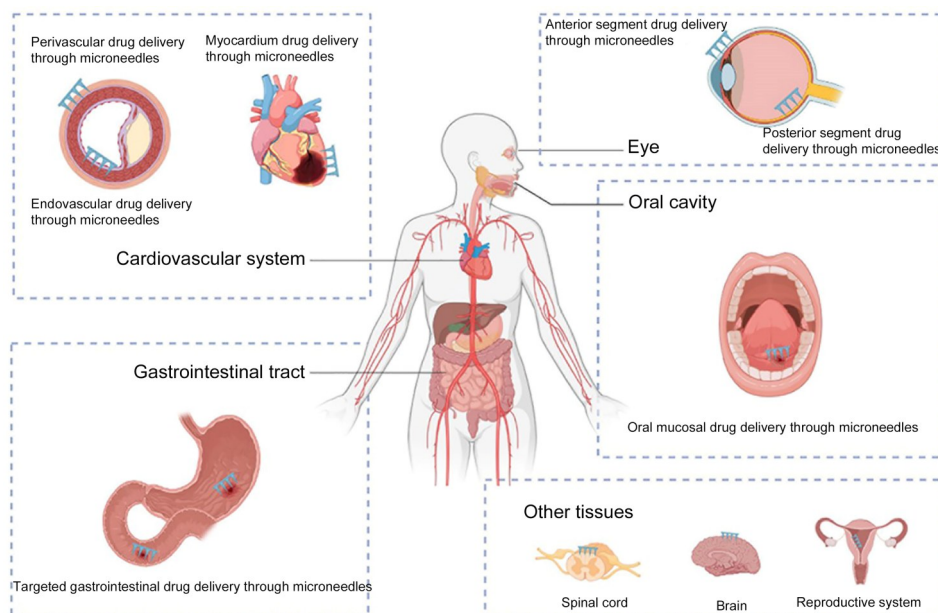


Fig. 2 Tissues for non-transdermal drug delivery using microneedles

diverse morphology of MN-related devices. To overcome anatomical complications and various physical properties of organs and tissues, sophisticated methods are often used in the fabrication of MNs to obtain optimal properties, such as mechanical strength, biodegradability, and biocompatibility, for the intended applications and significant advantages in bypassing drug resistance and minimizing detrimental side effects.

2.1 Materials

Different types of materials have been used for MN manufacturing according to the corresponding requirements of different applications. Choosing the appropriate material is critical in designing non-transdermal MNs. Silicon [5, 15], silicon dioxide [16], ceramics [17], and metals, such as titanium [18] and stainless steel [19], were initially used to fabricate solid MNs, which simply open pores on the skin to promote drug permeation because of their high stiffness. These nondegradable materials are also preferred for hollow and coated MNs. Compared with metals, polymers enable controllable drug release and are biodegradable. MNs fabricated from polymers can be designed to dissolve after insertion into the body [20, 21]. Carbohydrate-based materials, such as trehalose, chitosan, maltodextrin, cellulose, glucose, hyaluronic acid (HA), and carboxymethylcellulose (CMC), have been widely used to create dissolving MNs, among which CMC and HA are the most frequently used. CMC is a biocompatible, biodegradable structural polymer that is often added to the matrix solution to increase viscosity. HA is a crucial element of the extracellular matrix and cartilage, which exhibits high biocompatibility and ideal mucoadhesive properties. In addition, high-molecular-weight HA (>50 kDa)

is immunosuppressive in vivo, whereas low-molecular-weight HA (<50 kDa) has no side effects, although it is proinflammatory [22, 23]. Synthetic polymers, such as polycarbonate, polymethyl methacrylate, polylactic acid (PLA), polyglycolide acid (PGA), poly(lactic-co-glycolic acid) (PLGA), polyvinyl acetate (PVA), and polyvinylpyrrolidone (PVP), have also been extensively used in fabricating MN-based drug delivery systems [24–26]. Because both PVA and PVP exhibit rapid dissolution when coming in contact with interstitial fluid and are mechanically robust enough to bear the insertion force required for tissue penetration, they meet all the criteria for the fabrication of advanced dissolving MNs and have thus been most commonly used as the fabrication matrix. The controlled release of drugs over time can be achieved via manipulating the degradation of polyesters, for example, by varying the ratio between PLA and PGA in the PLGA copolymer [27]. These polymers are expediently available and do not require complex preparation for use; therefore, they are likely to be introduced into industrial production lines and may soon facilitate large-scale manufacturing. Another novel material used in fabricating dissolving MNs is silk fibroin, which is obtained from *Bombyx mori* silkworm cocoons. Fibroin can enhance the mechanical strength and robustness of MNs, and its customizable properties enable a sustained drug release profile [24]. In addition, by adjusting crosslinking methods and chemical modification techniques, polymers can be fashioned into hydrogels and mixed with different types of drugs, including small molecules, macromolecules, nanoparticles, and nucleic acids, to fabricate swellable MNs. Hydrogels, such as poly(ethylene glycol) diacrylate, Gantrez S-97, Gantrez AN-139, gelatin methacryloyl

(GelMA), and methacrylate HA are typically biocompatible and often have relatively low mechanical properties and faster degradation, which are ideal for rapid drug release. Hydrogels could also be designed accordingly for controlled drug release corresponding to the drug size. Adjusting the weight percentage of the crosslinker or the molecular weight of the crosslinker itself to alter the crosslinking density may lead to changes in swelling ability. A more rapid swelling of the hydrogel results in a more rapid drug release [28, 29].

2.2 Fabrication techniques

With the increased variety of available materials and continuous development of microprocessing technology, the manufacturing of MN arrays has also expanded from the conventional microfabrication technique to other more advanced technologies, such as three-dimensional (3D) printing, drawing lithography, and multistep micromolding. These strategies enable a high flexibility in the morphology of the needle tips during the fabrication process.

2.2.1 Microfabrication

Since the first report on the application of MNs, which were developed from silicon using deep reactive ion etching (DRIE) [5] for drug delivery, traditional silicon manufacturing technologies, such as photolithography and dry and wet etching, were subsequently introduced into the fabrication process. Currently, these microfabrication methods, which employ microelectromechanical system technology, have been widely used in the fabrication of both in-plane and out-of-plane MN arrays, which serve as ideal gateways for achieving highly efficient but cost-effective production [30].

In general, dry etching techniques can be categorized into plasma etching, reactive ion etching, and ion milling based on the process pressure differentiator during fabrication. The most common dry etching process is DRIE, commonly known as the Bosch process [31]. DRIE features highly anisotropic silicon etching with high selectivity and enables desired MN applications with especially high aspect-ratio features and smooth vertical sidewall geometries to be achieved by controlling parameters, such as gas flow rates, etch pressure, temperature, power and bias, and the type of masking layer. Wet etching can be classified into different types according to the aqueous etchants used, which include tetramethylammonium hydroxide (TMAH), ethylenediamine pyrocatechol, potassium hydroxide, hydrofluoric acid, and HNO₃. For either isotropic (the etch rate is the same in all directions) or anisotropic (the etch rate differs for different crystal planes) etching, the etch rate of the etchant material chosen should be greater than that of the etch mask material so that the exposed position can be

dissolved and then removed [32, 33]. Wet etching can be used to fabricate MNs with different aspect ratios that enable targeted drug delivery depths [15, 34]. Hamzah et al. [35] demonstrated that a high aspect ratio can be obtained under optimal production parameters by aligning the surface of the sample perpendicular to the etchant flow direction. Although wet etching is generally faster and more cost-effective than dry etching, it cannot be effectively applied to produce high-aspect-ratio boreholes for hollow MNs. Indeed, hollow-structured MNs with flow channels can be fashioned using combined wet and dry etching steps, during which front DRIE and rear DRIE form the pillar structure, while wet etching refines and sharpens the pillars to needles [31, 36, 37]. The photolithographic approach is usually used in the fabrication of polymeric MNs. Template etching can be achieved by covering the target substrate with a specific photoresist and then exposing it to ultraviolet radiation (Fig. 3a) [38]. By combining single-step photolithography and etching, solid MNs with high aspect ratios can be manufactured. Pradeep Narayanan and Raghavan [39] produced tapered MNs with sharper tips. During the process, single-step lithography and anisotropic TMAH wet etching techniques were incorporated to obtain a high aspect ratio and successfully increase the insertion length of MNs designed with sharper tips and unique geometry. Roh et al. [40] proposed a fabrication method combining single-step photolithography and two subsequent DRIE steps using dumbbell well photomask patterns. They successfully obtained high-density, out-of-plane MNs with various lengths and diverse cross-sectional shapes that could reach adequate penetration depths into the skin or brain to promote more effective drug delivery and advance neurophysiological studies.

2.2.2 Photopolymerization-based 3D printing

3D printing is a rapid additive manufacturing method that is mainly classified as photopolymerization- or extrusion-based 3D printing [41, 42]. Photopolymerization-based techniques have recently attracted extensive attention because of the simple preparation process, short preparation period, high preparation precision, and considerable freedom in structure design. During fabrication, the introduction of photo-crosslinkable biomaterials with enhanced physical and chemical properties enables rapid gelation upon exposure to light irradiation in the presence of photoinitiators. Photopolymerization-based 3D printing can be further divided into point-by-point printing, including stereolithography (SLA) and two-photon polymerization (TPP), and layer-by-layer printing, such as digital light processing (DLP) (Fig. 3b). In SLA, a computer-controlled ultraviolet (UV) light beam is used to induce the point-by-point polymerization of photosensitive resins and then deposit them on the material surface. By adjusting the irradiation

area, illumination time, and UV light intensity, MN arrays with different shapes can be prepared [43]. Compared with SLA, TPP allows for a higher resolution and better printing accuracy in creating 3D structures through the simultaneous absorption of two or more photons and likewise enables the point-by-point solidification of photosensitive materials. TPP enables the relatively simple production of complex structures [44]. Cordeiro et al. [45] reported that TPP serves as a flexible and reliable approach to manufacturing MNs that are fully conical or pyramidal, cuboidal (base)/pyramidal (tip), and cross-shaped. Furthermore, such MNs demonstrated high drug delivery rates *ex vivo* and *in vitro*. In addition, hollow MNs with various hole structures and MNs with open microfluid channels can be easily fabricated using TPP [46, 47]. During DLP, the geometry of the needle is shaped by solidifying the photosensitive resin layer by layer using a digital micromirror device. Parallel printing is performed by projecting the entire plane of the optical pattern onto the photopolymer solution, thereby enabling fast but cost-effective preparation. The printer resolution is at the micron scale, which is determined by the focal size of the light beam from each micromirror [48]. Because of these advantages, DLP is a potential method for constructing the finer surface microstructures of needle bodies, as well as fabricating in-plane and out-of-plane hollow MNs with different aspect ratios.

The concept of four-dimensional (4D) printing has been proposed to better match native tissue dynamics and meet shape changes. By extending the 3D space into the fourth dimension which is time, the development of biomaterials and bioinks can be continually customized. Constructed of active/smart materials with the ability to self-assemble, self-heal, self-reproduce, and retain shape, the production process can be preprogrammed and adjusted to achieve more native-like results, which adequately satisfies the functional requirements of MN applications for non-transdermal drug delivery [49]. 4D printing has been successfully applied to new regenerative therapies for cardiovascular diseases. Bio-mechanical adaptive heart patches successfully manufactured using this technology can attach to the tissue surface and repair the injured myocardium [50, 51].

2.2.3 Drawing-based technologies

Novel dissolving, drawing-based MN fabrication techniques provide different choices for the manufacture of MNs for non-transdermal drug delivery. Thermal drawing, a drawing lithographic method that allows a 3D structure to be directly formed from 2D materials, is commonly used in the construction of polymer MNs with high aspect ratios. The heated viscous polymer is vertically drawn by a metal micropillar at a regulated speed and then undergoes a rapid lift after a cooling step to fracture the

narrow neck microstructure and form the MNs [52]. During the continuous fabrication process, the viscosity of the drawn polymer can be controlled by adjusting the temperature and drawing points in the glass transition history of the polymer materials, which controls the extensional deformation, to precisely modulate the tip geometry (Fig. 3c) [53]. However, this might also result in the formation of irregularly structured MNs with either a cylindrical or bar shape [54]. Therefore, a stepwise, controlled thermal drawing method is performed to avoid the development of unsuitable shapes, through which particular MNs with sharp tip ends can be correspondingly created. Lee et al. [55] proposed a three-step thermal drawing technique, composed of contact, body, and tip drawing, which can rapidly manufacture polymer MNs with various shapes on various surfaces. MNs with various features were manufactured based on temperature-dependent polymeric behavior and controlling thermal mapping parameters. During the drawing process, the final shape of a single needle could be variably determined by the temperatures of the micropillar and substrate (temperatures at boundaries of the drawn polymer) and dwell time. The change in temperature could influence the polymer chain mobility at each local point of the drawn polymer. In particular, when the temperature was adjusted from low to high, the aspect ratio increased correspondingly. The aspect ratio also increased with the extension of dwell time. Based on the conventional three-step thermal drawing method, transfer thermal drawing was then proposed to produce MNs on different substrates.

Other drawing-based technologies, such as electro-drawing, droplet-born air blowing (DAB), and magnetorheological drawing, can also be applied to MN fabrication. Electro-drawing has been proposed as a contact-free process without the use of UV light for the manufacturing of polymer MNs, such as PLGA-based MNs (Fig. 3d) [56, 57]. DAB is an advanced method with a simple process, gentle fabrication conditions, low cost, and massive productivity. DAB enables the polymer droplet to solidify immediately into the required MN shape within 10 min. The quick fabrication preserves the biological activity of the loaded drugs (Fig. 3e) [58]. Magnetorheological drawing lithography (MRDL) is a rapid and easy fabrication method that eliminates the need for a mask, light irradiation, and drawing temperature adjustment. In MRDL, droplets of curable magnetorheological fluid can be drawn directly from almost any substrate to produce various MN tip structures under an external magnetic field. A tilted MN can also be fabricated by altering the direction of the magnetic field, by which the tilt angle of the needle tips can be adjusted [59, 60]. As a 3D manufacturing process, MRDL can be used to produce complex bio-inspired microstructures, such as tilted microbarbs, which facilitate easy skin insertion but difficult removal (Fig. 3f) [61].

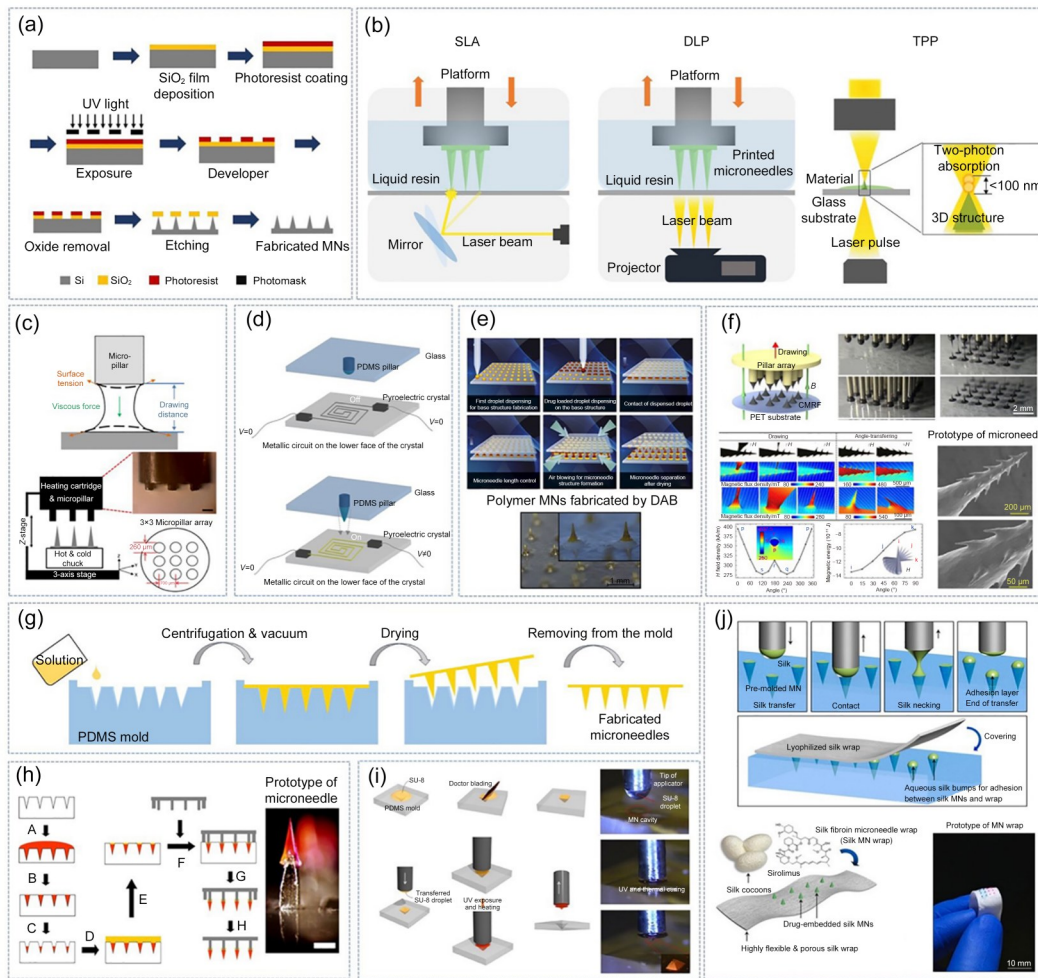


Fig. 3 Various methods for fabricating microneedles (MNs). (a) Typical microfabrication method through etching. (b) Photopolymerization-based 3D printing including stereolithography (SLA), digital light processing (DLP), and two-photon polymerization (TPP). (c) Schematic diagrams of the thermal drawing process (Reprinted from [55], Copyright 2019, with permission from the authors, licensed under CC BY 4.0). (d) Schematic diagram of the electro-drawing process (Reprinted from [57], Copyright 2017, with permission from Elsevier B.V.). (e) Schematic diagram of the droplet-born air blowing process (Reprinted from [58], Copyright 2013, with permission from Elsevier B.V.). (f) Steps of fabrication by magnetorheological drawing lithography (Reprinted from [59], Copyright 2019, with permission from the American Chemical Society). Microbarbs on the parent MN can be shaped through this method, and the tilted angles can be adjusted using the magnetic field (Reprinted from [61], Copyright 2018, with permission from the American Chemical Society). (g) Steps of the conventional micromolding method. (h) Fabrication progress of MNs manufactured through multistep molding with a prototype of a single needle (scale bar, 300 μ m; Reprinted from [71], Copyright 2010, with permission from Elsevier B.V.). (i) Fabrication of an MN pen manufactured through the transfer molding method (Reprinted from [72], Copyright 2015, with permission from Elsevier B.V.). (j) Fabrication progress of a trappable silk MN mesh manufactured using the transfer molding method (Reprinted from [74], Copyright 2021, with permission from Elsevier B.V.).

2.2.4 Molding techniques

In addition to these diverse and complicated manufacturing techniques for directly constructing MN structures, micromolding methods further increase the options (Fig. 3g). In the micromolding process, patterned polydimethylsiloxane (PDMS) is used as a mold for substrates [62]. PDMS molds with different microchannel geometries can be directly formed using laser technology [63–65] or through multistep casting after defining the multiform microfluid by lithography [66, 67] or 3D printing [68]. PDMS is then poured over to obtain the negative mode structure. MNs with specific

functions can then be customized by filling the shaped cavities with the biomaterial solution. Correspondingly, single or composite materials are selected for MN preparation according to the requisite mechanical strength and solubility properties. Based on the micromolding method, the solidification of the polymeric solution or melt enables MNs to stably bind on a macroscale structure, which facilitates a wide range of applications, such as separable MNs, MN pens, and MN meshes. Several studies have developed separable MNs constructed using a PVA/PVP soluble base and drug-loaded tips with certain biofunctions via a two-step

molding technology. The dissolution of soluble supporting bases after absorption of tissue fluid allows the separable MN arrowheads to be inserted and embedded into the skin [69, 70]. In the study by Chu and Prausnitz [71], the MN arrowheads were first formed in micron cavities and then connected to the backing shaft arrays under gentle force, which embedded the MN shafts into the base of the arrowheads. After drying/solidification, the arrowheads were removed from the mold to yield a complete MN patch (Fig. 3h). Similarly, the method can be used in the fabrication of different MN pen applications. SU-8 droplets were used as the junction of MN tips and pen substrate, which were solidified under heating and UV curing (Fig. 3i) [72, 73]. Wrappable MN mesh applications for perivascular drug delivery using the transfer molding method have been described. Drug-embedded material was poured into the PDMS mold, and an adhesion layer was created above the MN cavities. A heated micropillar was then used to melt the adhesion layer after attaching the flexible mesh to the needle tips to complete the assembly of the MN mesh upon cooling (Fig. 3j) [74, 75].

3 Special design strategies for non-transdermal drug delivery

When administering drugs, lesions in different nondermal tissues require corresponding therapeutic criteria and specific dosing strategies. MNs used for treatment should remain closely attached to the tissue and degrade over time to allow the loaded drugs to be released safely and sustainably. For diseases that require long-term treatment or those that require periodic administration, smart MNs with controlled drug release need to be developed. By selecting appropriate methods for the precise control of the morphology and structure, different forms of MN-based drug delivery devices with ideal mechanical properties can be manufactured to carry specific biomolecules for curing and monitoring diseases [76].

3.1 Safety considerations

3.1.1 Biodegradability and biocompatibility

Because MNs will come in contact with interior organs and tissues, the biosafety and biosecurity of their applications must be determined. Given the considerations of bioavailability and drug release efficiency, biodegradable and bioabsorbable materials may be the essential choice for medical applications, including MNs for therapeutic use [77]. Evaluation of degradation for *in vitro* and *in vivo* experiments should be conducted to characterize the biodegradability of MNs. Biocompatibility not only means that the

biomaterials would not elicit any adverse local or systemic reactions, such as inflammation, edema, and other pathological changes, when applied, but also indicates the nontoxicity of the degradation byproduct, which should not cause detrimental side effects with accumulation. Furthermore, the materials should exhibit sustained release capability with long-term anti-inflammatory effects [78, 79]. *In vitro* cell experiments are often performed for evaluation, in which cells are cocultured with the MNs, and then cell viability and proliferation are assessed. Overall evaluation of tissue pathology and systematic hematologic and biochemical analyses *in vivo* are also needed to evaluate for side effects in response to the implantation of MN devices.

3.1.2 Self-locking for secure fixation

The basic consideration of efficient drug delivery to nondermal tissues involves smart designs of the fastening of MNs to various surface environments to prevent dislodgment and potential injury. Inspired by natural bio-MNs, the structures of needle tips can be manufactured into various configurations that feature optimal geometry and possess excellent tissue fixation performance, mainly due to the intelligent combination of microstructures and insertion modes [80]. For example, MNs with replicated angled tips would keep the patch firmly adherent when the attached substrate moved and rotated or was placed under external forces. Zhang et al. [81] designed a serrated clamping MN array based on ferrofluid-configured moldings. The high adhesive ability of the tilted MNs was attributed to the increased grasping force created by the centrally oriented structures of the serrated clamping array (Fig. 4a). In a subsequent study, the team fabricated clamp-structured MNs in another device for linear wound healing [82]. Another approach to constructing “array in array” needle tips may also increase the tissue adhesion capability of MNs. Inspired by natural honeybee stingers that generate higher interlocking strengths at the cross-sectional area of the contact point, a tip structure with an array of barbs localized in the second half of the MN cone has been proposed [61]. Lu et al. [83] fabricated bio-inspired self-interlocking MN patches with backward-facing barbs. Patch interlocking and adhesion in tissues were confirmed by optical coherence tomography, mechanical tests, and *in vivo* experiments (Fig. 4b). In addition, sufficient tissue adhesion ability can be achieved through many other forms of microstructure surfaces. Liu et al. [84] fabricated a porcupine quill-like multilayer MN patch with an adhesive hydrogel back patching by layer-by-layer stacking using mold technology. The extra area generated at the junction of the two adjacent layers of the MNs ingeniously created a barb-like structure, which contributed to enhanced MN adhesion (Fig. 4c). In addition, swellable MNs using

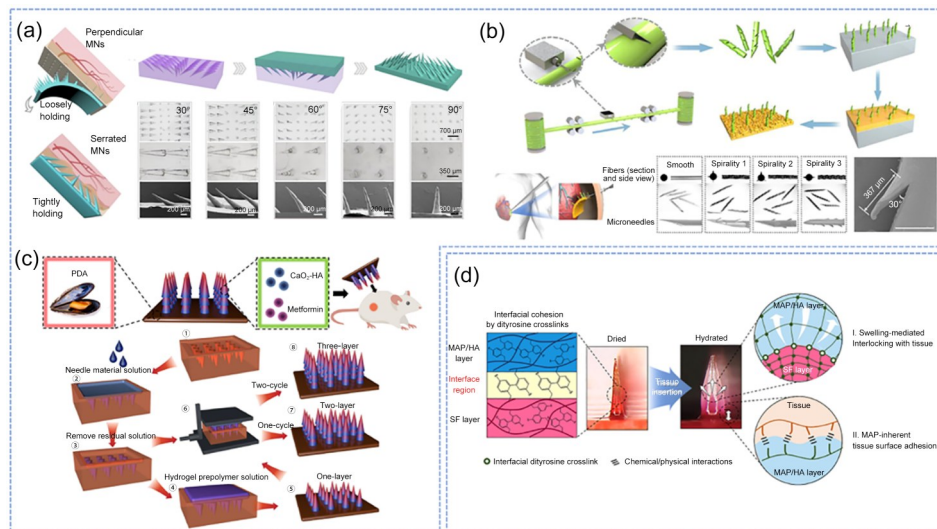


Fig. 4 Schematic diagrams of microneedles (MNs) used to achieve secure tissue fixation. (a) A clamping MN array with center-facing tilted needles (Reprinted from [81], Copyright 2019, with permission from Science China Press). (b) An MN patch with backward-facing barbs that enables self-interlocking in heart tissue (Reprinted from [83], Copyright 2022, with permission from Acta Materialia, Inc.). (c) A self-locking structure MN patch fabricated via layer-by-layer stacking (Reprinted from [84], Copyright 2023, with permission from Acta Materialia, Inc.). (d) Swellable hydrogel materials that enhance MN adhesion (Reprinted from [87], Copyright 2019, with permission from Elsevier Ltd.)

materials that allow the expansion of the polymer network structure after tissue fluid diffuses into the MNs are a promising option for mechanical interlocking with tissue (Fig. 4d) [85–87]. The prepared arrays mentioned above have great potential as excellent drug-release devices with ideal attachment capability, further expanding the possibilities for the biomedical application of MNs.

3.2 Strategies for achieving controlled drug release

3.2.1 Long-term drug release

Dissolving MNs have mainly been investigated for drug delivery because of their fully water-soluble design. Long-term release MN patches can be designed using multilayer-coated structures, which are remarkably functional due to distinctive advantages that include various drug loading possibilities and regulation of drug release behavior. By adjusting the coating composition film by film, the release curve of vaccine components can be flexibly adjusted. Uppu et al. [88] produced MNs with polymer multilayer thin films to co-deliver a model combination of three chemically distinct vaccine components. The MNs facilitated the sustained and rapid release of individual vaccine components from polymer multilayers by implanted thin films. By modulating layer-by-layer composition and architecture, components in the MNs could be independently controlled to release over the course of days up to two weeks (Fig. 5a).

The fabrication of detachable MNs follows the principle of making the backing layer separable from the needle tips,

which promotes the proper insertion or implantation of MNs loaded with drugs into the skin for long-term delivery. Various applications can be designed by utilizing different mechanisms for backing layer separation. By capping drug-loaded dissolving needle tips onto a solid base without the drug via multistep molding fabrication, rapid separation can be achieved (Fig. 5b) [70]. Alternatively, easy separation can be implemented by using an intermediate to connect the tips and the backing that possess disparate mechanical properties. Jung et al. [89] developed a separable micropillar integrated dissolving MN which can be inserted or detached immediately. The micropillars were fabricated with a diameter of 500 μm and a curved edge, while the base diameter of the MNs was 300 μm , which created a 200- μm safety ring over each micropillar, ensuring that only the dissolving MNs penetrated the skin. The patch could then be separated by applying a lateral force (Fig. 5c). Li et al. [90] demonstrated the rapid separation of MNs after inserting them into the skin by constructing an air bubble between the backing layer and MNs using the two-step micromolding method. The air bubbles tolerated sufficient stress, allowing MNs to efficiently penetrate the skin under vertical compression while remaining easily detachable under modest shear force, resulting in MNs separating from the patch matrix and becoming implanted into the skin. The same performance can be achieved by introducing a porous interface between MNs and the backing layer. Lee et al. [91] fabricated an MN patch with a porous interface between needle tips and a patch backing made of PVP/sucrose, which enabled complete separation within 1 s after skin insertion due to the fragile character of the lyophilized porous interface between

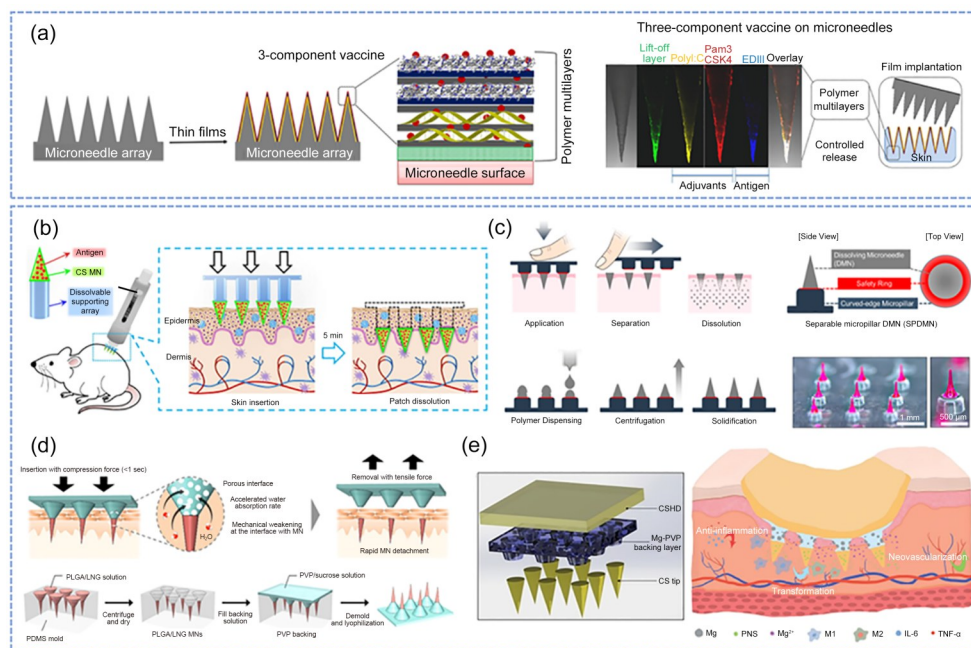


Fig. 5 Schematic diagrams of microneedles (MNs) for achieving long-term drug delivery. (a) Multiple film coatings (Reprinted from [88], Copyright 2020, with permission from Elsevier B.V.). (b) Detachable MNs with supporting array (Reprinted from [70], Copyright 2017, with permission from Acta Materialia, Inc.). (c) Separable MNs with micropillars (Reprinted from [89], Copyright 2020, with permission from the authors, licensed under CC BY 4.0). (d) MNs with a porous interface for rapid detachment after application to tissue surface (Reprinted from [91], Copyright 2021, with permission from Elsevier B.V.). (e) Detachable microneedle with multiple layers (Reprinted from [92], Copyright 2022, with permission from Wiley-VCH GmbH)

the tips and patch backing (Fig. 5d). In addition, by constructing a synergistically separable system with a multi-layer structure, detachable MNs can be developed. Ning et al. [92] proposed a dual-layer dressing MN system by adding an Mg/PVP layer, which would accelerate separation and promote drug release. In the experiment, H_2 was generated by the reaction between Mg and the inflammatory microenvironment, forming air cavities in the Mg/PVP layer, which increased the reaction area, accelerated the dissolution of PVP, and then enabled synergistic detachment of MNs and continuous drug release (Fig. 5e).

3.2.2 Multistage drug release

Multistage drug release can be achieved by integrating well-characterized controlled-release microspheres and microparticles made of hydrophobic biodegradable materials with dissolving MNs [93–96]. To increase vaccination safety and coverage, Mazzara et al. [97] explored controlled-release PLGA microparticles that could stably encapsulate various antigens via aqueous active self-healing encapsulation (ASE). The microparticles were then incorporated into rapid-dissolving MNs for vaccination. The study designed a new platform with multiple advantages over traditional vaccine delivery strategies, which could perform controlled antigen release via PLGA MNs while maintaining antigen stability by avoiding antigen exposure to protein-damaging

stresses. This MN patch demonstrated bi-phasic release in vitro with an initial burst of soluble antigen followed by delayed release over approximately two months to generate more robust immune responses than conventional vaccines in animal models (Fig. 6a).

Given their stable mechanical properties and programmed drug delivery, core–shell structure MNs have become more reliable and suitable tools for efficient self-administration. Tran et al. [98] proposed a core–shell microstructured MN, including an MN shell, MN cap, and a dried drug or vaccine core. The MNs were generated through a 3D manufacturing process that assembled the three components. The drug or vaccine core was encapsulated by a cap and base layer composed of PLGA. By tailoring the degradation of the PLGA shell, precisely controlled drug release was achieved. In the clinical setting, multiple sets of MNs with different PLGA shells could be simultaneously inserted into the skin to achieve multiple burst releases after different durations to achieve an effect similar to multiple drug injections. Li et al. [99] created a superior constant-release system of levonorgestrel (LNG) that lasted for six months based on a core–shell–cap structure. The release time was three times longer than that of MNs with a monolithic core but without a surrounding shell. In this work, LNG was incorporated into a monolithic core made of biodegradable PLGA, with an estimated degradation of less

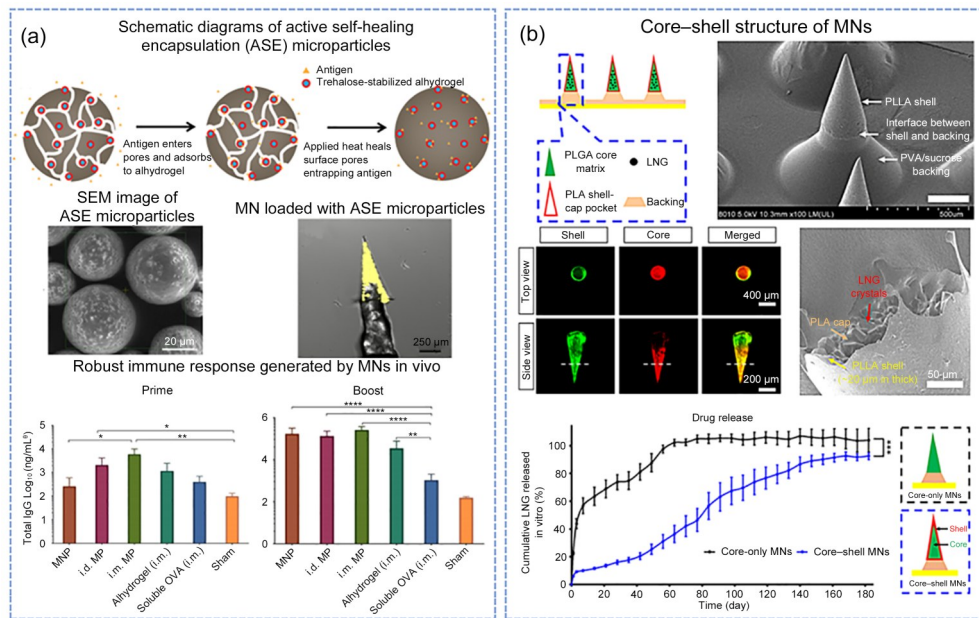


Fig. 6 Schematic diagrams and prototypes of microneedles (MNs) used for multistage drug delivery. (a) Dissolving MNs loaded with poly(lactic-co-glycolic acid) microparticles containing antigens (MNP: microneedle patch; i.d. MP: intradermal injection microparticle; i.m. MP: intramuscular injection microparticle; OVA: ovalbumin; Reprinted from [97], Copyright 2018, with permission from the authors, licensed under CC BY). (b) A core-shell structured MN patch for sustaining levonorgestrel release (Reprinted from [99], Copyright 2022, with permission from Elsevier B.V.)

than six months. The core was surrounded by a shell and cap layer made of PLA, which had an expected degradation of more than six months to minimize initial burst release and provide a slower, more constant drug delivery (Fig. 6b).

3.2.3 Responsive drug release

Stimulus-responsive MNs have been fabricated from specific polymer materials that are capable of responding to changes in the surrounding environment to achieve controlled and programmed drug release. Physiological signals, such as near-infrared (NIR), and internal stimuli, such as pH, redox potential, glucose, and enzymes, are potential triggers that can induce MN responses, such as matrix degradation and matrix swell [100]. pH-responsive MNs often consist of polymers containing hydrophilic and ionic functional groups in the polymer segments. Drugs can be released upon matrix disassembly or dwelling associated with pH changes [101]. Low pH in chronic wound and inflammation sites is the most common stimulus for designing pH-sensitive drug delivery systems [102, 103]. For example, an MN system loaded with micelles formed by the self-assembly of a pH-responsive tri-block polymer (DMA-PEI-PLGA, DPP) and Ce6-coupled antimicrobial peptide sequence (AMP-Ce6, AC) has been fabricated for the controlled release of antimicrobial drugs in the skin [104]. The acidic environment protonated the hydrophobic PLGA block tertiary amine to become

hydrophilic, which then caused the disintegration of the micelle and the subsequent release of the positively charged DMA group, thereby significantly improving the specific bacteria-targeting ability of the antimicrobial peptide (Fig. 7a). In addition, because the microenvironments of most tumors have a pH that is lower than that of non-cancerous tissues, pH-responsive MNs have significant practical implications in cancer therapy [105]. In a study, a pH-responsive polymer underwent charge conversion upon exposure to the acidic tumor microenvironment, causing the polymeric layers to swell and the gene cargos to be released, thereby achieving efficient targeted delivery of antitumor therapeutic agents [106] (Fig. 7b).

Closed-loop systems based on MNs have become a novel method for glucose-responsive insulin delivery, which eliminates the need for patients with diabetes to voluntarily inject insulin. The glucose sensing function of these devices can be accomplished via several approaches, including glucose oxidase (GO_x)-catalyzed environmental changes [107], glucose-binding molecules, and glucose-detecting compounds-mediated molecular recognition [100]. GO_x-catalyzed pH decrease [108], O₂ consumption (hypoxia), and H₂O₂ generation [109, 110] are most frequently applied as triggers for glucose-responsive MNs (Figs. 7c and 7d). MNs based on specific glucose-sensitive molecules have also been used in self-regulated insulin delivery. Yu et al. [111] introduced a phenylboronic acid (PBA)-based glucose-responsive MN system for the experimental treatment of diabetes. When

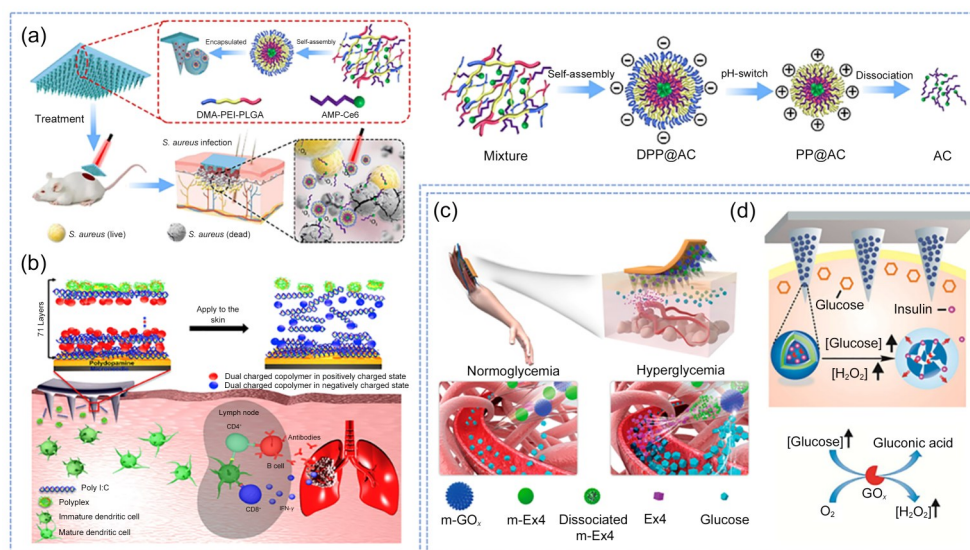


Fig. 7 Schematic diagrams of microneedles (MNs) for achieving internal stimulus-responsive drug delivery. (a) A pH-responsive MN patch for wound healing (Reprinted from [104], Copyright 2023, with permission from Elsevier B.V.). (b) A pH-responsive MN patch for vaccine delivery in cancer therapy (Reprinted from [106], Copyright 2018, with permission from Elsevier Ltd.). (c) A glucose-responsive MN patch loaded with dual mineralized particles (Reprinted from [108], Copyright 2017, with permission from the authors, licensed under CC BY 4.0). (d) Glucose-responsive MNs for insulin delivery induced by H₂O₂-sensitive GO_x particles (Reprinted from [110], Copyright 2017, with permission from the American Chemical Society)

exposed to a hyperglycemic state, the formation of glucose–PBA complexes increased negative charges and weakened the electrostatic interaction between negatively charged insulin and polymers. This induced volume variation in the polymeric matrix, resulting in the quick release of insulin from the MNs. Once the blood glucose level returned to normal, volume variation became inhibited, and the electrostatic interaction was restored, thereby slowing down insulin release to avoid causing hypoglycemia.

4 Advanced applications in different tissues

Non-transdermal MNs can deliver drugs to various tissues that have moist, dynamic tissue environments. Unlike those implemented on flat, dry, and easy-to-handle skin surfaces, non-transdermal MNs require more consideration to surmount multiple barriers. Various organizational applications can be classified according to the properties of the local environment, surface characteristics, organ activity, and mechanical properties.

4.1 Cardiovascular system

Cardiovascular diseases (CVD) including myocardial infarction, stroke, and peripheral vascular disease, are the leading causes of death worldwide [112]. MNs have been found feasible for the treatment of CVD. However, the cardiovascular system is a wet, dynamic, and pressurized system,

making it a challenging environment for the application of MNs.

Atherosclerosis is a high-risk factor for CVD [113]. Vascular bypass and insertion of drug-eluting stents (DES) are the most common clinical interventions for atherosclerosis. However, some patients may develop neo-intimal hyperplasia (IH) at the surgical site postoperatively. Current research on vascular drug delivery is mainly aimed at delivering anti-proliferative drugs, such as sirolimus or paclitaxel, to investigate the prevention of IH [114–116]. Considering that the structure of vascular vessels is composed of three layers (tunica adventitia, tunica media, and tunica intima), perivascular drug delivery through the adventitia and endovascular drug delivery through the endothelium are potentially the most viable drug delivery strategies.

4.1.1 Perivascular drug delivery

Because of the elastic characteristics of blood vessels and blood pressure fluctuations, a rigid perivascular drug delivery device may cause abnormal proliferation of smooth muscle cells in the blood vessels and exacerbate the problem of secondary stenosis of blood vessels. Thus, devices with curved substrates that could exert their drug delivery mechanism by wrapping around the vascular structures were then proposed. Over the past decades, meshes, wraps, sheaths, and cuffs have been proven safe and feasible in perivascular drug delivery [117]. By introducing MNs to the flexible substrates of these devices, closer adhesion between wraps and vascular surfaces may be achieved, resulting in

enhanced drug delivery efficiency. Choi et al. [118] designed a drug-loaded MN cuff that was successfully inserted through the tunica adventitia to deliver the fluorescent molecule rhodamine B as a model compound to the tunica media. The curved patch base is made of a relatively slow-degrading polymer, and the curvature was developed by post-annealing inside a cylindrical stainless tube at 72 °C. Lee et al. [119, 120] further increased the drug delivery efficiency to the inner layers of vascular tissue by installing the MN structure onto the cuff surface and confirmed the therapeutic effect in subsequent in vivo experiments. In 2017, Lee et al. [75] proposed a biodegradable PLGA80/20 MN array developed on a flexible woven surgical mesh via a transfer molding method. Enhanced drug delivery efficiency, efficacy in IH reduction, safety of the MN mesh, and minimal side effects were demonstrated ex vivo and in vivo (Fig. 8a). Later in 2021, the team developed a

highly flexible and porous silk fibroin MN wrap that directly injected an antiproliferative drug into anastomosis sites while ensuring sufficient vascular exchanges [74]. The results of in vivo studies on New Zealand white rabbits confirmed that the silk MN wrap showed superior pharmaceutical efficacy compared with drug-loaded silk wrap without MNs, with enhanced perivascular drug delivery efficacy for IH reduction, improved vessel patency, and the maintenance of a healthy tunica media layer. The remarkable flexibility due to the structural characteristics of the mesh substrate indicates the potential application of such MN-based devices for perivascular drug delivery in blood vessels with complex shapes and various sizes (Fig. 8b).

Because MNs are applied to the outer surface of the blood vessel, invasive surgeries are unavoidable during implantation. Surgical risk may be a major limiting factor that should be addressed in further research. Therefore, minimizing

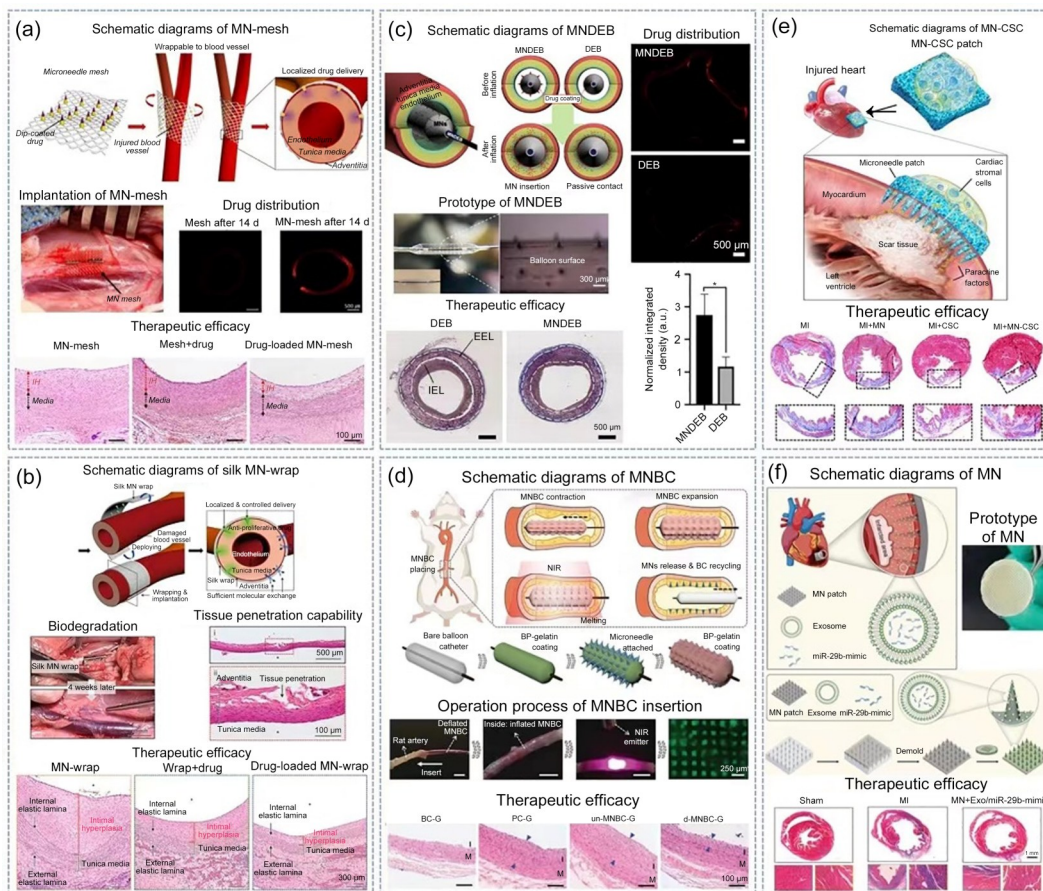


Fig. 8 Microneedle (MN)-based applications for cardiovascular drug delivery. (a) Biodegradable MN array developed on a flexible woven surgical mesh for perivascular drug delivery (Reprinted from [75], Copyright 2017, with permission from Elsevier B.V.). (b) Highly flexible and porous silk fibroin MN wrap for perivascular drug delivery (Reprinted from [74], Copyright 2021, with permission from Elsevier B.V.). (c) An endovascular MN drug-eluting balloon for endovascular drug delivery (Reprinted from [124], Copyright 2020, with permission from Elsevier B.V.). (d) NIR-triggered intelligent MN balloon catheters for endovascular drug delivery (Reprinted from [125], Copyright 2022, with permission from the authors, licensed under CC BY). (e) MN patch loaded with cardiac stromal cells for treating myocardial infarction (Reprinted from [127], Copyright 2018, with permission from the authors and exclusive licensee American Association for the Advancement of Science). (f) MNs loaded with exosomes containing microRNA-29b for cardiac tissue regeneration (Reprinted from [131], Copyright 2023, with permission from Wiley-VCH GmbH)

surgical injuries and properly monitoring the effects of MN degradation and drug release in real-time without repeated operations are worthy prospects for future studies.

4.1.2 Endovascular drug delivery

Current clinical trials, such as DES and drug-eluting balloons (DEB), have revolutionized the treatment of atherosclerosis in coronary and peripheral vasculature [121]. Various modifications to DEB aimed at improving the efficiency of endovascular drug delivery have been performed in recent years. Lee et al. [122] developed a linear micropattern-based DEB with 16 linear micropatterns on the surface, which successfully increased the contact force between the drug-coated surface and the lumen, thereby enhancing endovascular drug delivery efficiency. Another method of endovascular drug delivery is to establish a microinfusion system by combining a hollow needle with a balloon catheter [123]. When the catheter is opened, the needle extends out of the balloon and is used to inject drugs directly into the surrounding luminal tissue. The Bullfrog microinfusion devices were designed accordingly to facilitate better drug distribution through the luminal tissue. MN structures have also been introduced into DEBs by molding MN arrays onto the balloon surface to improve drug delivery efficiency. An MNDEB was fabricated via conformal transfer molding [124]. During the *in vivo* animal experiment, MNDEB was deployed in the iliac arteries in an atherosclerotic rabbit model. Compared with conventional DEB, drug-coated MNs molded onto balloon surfaces enhanced the efficiency of endovascular drug delivery, while maintaining the integrity of the vascular tissue despite MN insertion (Fig. 8c). Inspired by the changeable spiny and inflatable body of globefish, Zhang et al. [125] fabricated intelligent hierarchical balloon catheters with concealed MNs for the treatment of cardiovascular disorders. The MN balloon catheters (MNBCs) have three coatings outside the bare balloon catheter: two BP-encapsulated gelatin layers and MNs in between. After implantation, the MNBCs expand and fully come into contact with the tunica intima. The gelatin layers eventually melt under NIR, releasing MNs in the tissue. The bare balloon catheter is later recycled. The intravascular delivery of rapamycin to abdominal aortic restenosis in rat models using drug-loaded MNBCs demonstrated superior endovascular drug delivery and therapeutic efficacy, indicating its potential application in cardiovascular therapy (Fig. 8d).

When establishing a subsequent surgical scheme for endovascular drug delivery MNs, the current sophisticated methods using DEBs or intravascular stent implantation can be used for reference. The intervention path should be decided according to the lesion site and diameter, vascular flexibility, tortuosity of the target artery, structural

characteristics of DEB-based MNs, and surgical complexity. Future research should focus on conducting replicated *in vivo* experiments on large animals to establish systematic surgical implantation programs corresponding to specific lesion sites. The gradual transition from animal studies to clinical trials, as well as the evaluation of the therapeutic effects of endovascular MN products on humans, also urgently need to be addressed.

4.1.3 Cardiac tissue

Necrosis resulting from myocardial infarction (MI) generally cannot be treated. However, stem cell therapy has been shown to be effective in cardiac tissue regeneration. Intramyocardial injection allows stem or myoblast cells to be directly delivered to the infarct boundaries. However, the drug solution may be expelled via the contraction of the myocardium, which thus causes poor drug retention [126]. MN patches that can be tightly attached to the myocardial surface and precisely transport the therapeutic agent to the target area could be a potential solution. In 2018, Tang et al. [127] first described the use of MNs in the treatment of MI. MN-integrated cardiac stromal cells secreting heart regeneration factors were loaded onto the back of a PVA patch and diffused into the scar tissue. Enhancement of angiomyogenesis in a rat model and protection of cardiac function in a porcine model were observed (Fig. 8e). Hu et al. [128] developed a detachable MN patch that transported PLGA nanoparticles loaded with mesenchymal stromal cell-secreted factors into the myocardium, promoted the regeneration of cardiomyocytes, reduced cardiomyocyte apoptosis and fibrosis, and restored myocardial volume during the cardiac remodeling process. Many studies have also investigated MN-mediated gene delivery for myocardial disease treatment. The delivery of MNs carrying adeno-associated virus encoding the vascular endothelial growth factor (*VEGF*) gene improved heart function by enhancing *VEGF* expression, promoting functional angiogenesis, and activating the Akt signaling pathway [129]. Lim et al. [130] developed a double-layered adhesive MN delivering a bio-functional peptide (BFP) fused with a bioengineered mussel adhesive protein. BFP from four different sources was genetically fused to the C-terminus of bioengineered foot protein type 1 composed of 12 repeats of a decapeptide (AKPSYPPTYK). Yuan et al. [131] proposed a biocompatible gelatin-based MN patch that was fabricated to load exosomes containing microRNA-29b mimics that exhibited anti-fibrotic activity (Fig. 8f). All treatments showed distinct effects and provided potentially useful options for MI treatment.

Indeed, MN patches have demonstrated advantages in cardiac tissue regeneration after MI. However, further improvements are required. Because the heart is an internal organ, thoracotomy is inevitable for MN implantation.

During patch placement, a hand vacuum device is still required. Minimally invasive surgery could be a possible alternative to thoracotomy, which signifies that MNs must be small enough or have shape-retaining characteristics. Further studies may focus on the apparatus used for minimally invasive surgery.

4.2 Ocular tissue

Because of the presence of ocular barriers and clearance mechanisms, administering drugs safely and effectively to the eye is challenging. Traditional eye drops, gels, and ointments are the most common treatments. Unfortunately, these methods have low drug permeation, low bioavailability, and fast clearance caused by physiological processes, such as blinking and nasolacrimal drainage. Static barriers, such as the tear film, mucin layer, and cornea, also prevent the permeation of exogenous substances [132]. The posterior segment of the eye contains the sclera, choroid, Bruch's membrane, and blood-retinal barrier. Conventional posterior drug delivery is achieved by invasive injection directly through the sclera and into the vitreous humor. Such drug delivery methods can have severe side effects, including tissue damage, eyeball perforation, optic nerve injury, and intraocular infections [133]. Constant rotations of the eyeball and movements of eyelids also decrease the treatment efficiency. MN-based systems, as a noninvasive drug delivery system, have seen remarkable developments in ophthalmic treatment in recent years. The main aim of ocular drug delivery is to improve bioavailability by increasing diffusion across the cornea, conjunctiva, and sclera. Previous reviews have discussed hollow, coated, and dissolving polymer MNs that have demonstrated high permeation of the drug [134, 135]. Here, we mainly summarize the relatively new and reliable intraocular drug delivery MN products that have been validated *ex vivo* or *in vivo*.

4.2.1 Anterior segment of the eye

Drug delivery to the anterior segment of the eye is performed through intracorneal methods. The thin, unsupported structure of the cornea poses difficulty for MN puncture and retention. To better fit the spherical structure of the eyeball and insert the needle tips into the cornea, some MN patches assumed the semi-spherical design of contact lenses. Datta et al. [136] fabricated a polyvinylpyrrolidone MN patch with a convex curvature of 3.08 cm circumference, 3.85 mm sagittal height, and an array of 25 conical MNs by micromolding. The MNs completely dissolved in the cornea within 60 s of application. *Ex vivo* corneal permeation studies using porcine eye globes showed a disposition distribution of 45.5%, 29.1%, 8.3%, 5.2%, 3.0%, and 0.2% of loaded drug within the cornea, aqueous humor,

vitreous humor, sclera, and choroid–retinal complex, respectively. Roy et al. [137] fabricated an MN corneal patch with a concave design to mimic a commercially available contact lens and achieved firm placement on porcine and rabbit corneas (Fig. 9a). Regarding the depth of penetration, clinical findings indicate that the length of MNs should be matched to the maximum injection depth of the corneal epithelium, which ranges from 43 to 63 μm [135]. However, Than et al. [138] fabricated an eye patch bound to an array of detachable MNs that was 600 μm long with an insertion depth of approximately 150 μm . The MNs did not cause significant inflammation or angiogenesis in the mouse cornea.

Drug delivery through a single micron-scale needle has been suggested, considering that the use of patches on the ocular surface may potentially lead to hypoxia. Better performance of single MN insertion can be realized by combining it with an injection-assisting applicator [72]. Lee et al. [73] assembled a biodegradable MN tip and supporting base to form a hybrid detachable MN pen (d-MNP) by pressure-assisted transfer molding. When applied to the cornea, the spring-loaded pen platform instantaneously injected MNs via a spring-generated impact with an optimum dwell time of 10 s and a force of 13.74 N. The drug-loaded detachable tip was kept within the corneal tissue to enable sustained drug release for more than 9 d. The drug-carrying tip was thus delivered to the mouse cornea. Although the amount of drug contained was only 2.6 ng, it was sufficient to effectively reduce the progression of keratitis (Fig. 9b).

The limitations of the existing studies mainly lie in the lack of uniform regulations on puncture depth. Therefore, more *in vivo* studies are required to discuss the requirements of length and insertion depth of ocular MNs. Furthermore, whether the results of animal experiments on corneal penetration have therapeutic implications in humans still needs to be assessed in further confirmatory clinical tests.

4.2.2 Posterior segment of the eye

For posterior segment diseases that commonly require drugs to reach the macular or peripheral retina, intrascleral administration brings drugs closer to the target site, thereby providing effective drug concentrations for treatment. Roy et al. [137] demonstrated the efficacy of an MN scleral patch in delivering triamcinolone acetonide as a model molecule to the posterior segment of the eye. Wu et al. [139] developed a nanoparticle (NP)-loaded bilayer dissolving MN array, which was deemed to be biocompatible with retinal cells (ARPE-19). *Ex vivo* scleral distribution studies confirmed that NP-loaded MN arrays exhibited a longer lag time in the sclera and sustained the release of encapsulated drugs. The group then fabricated MNs loaded with triamcinolone

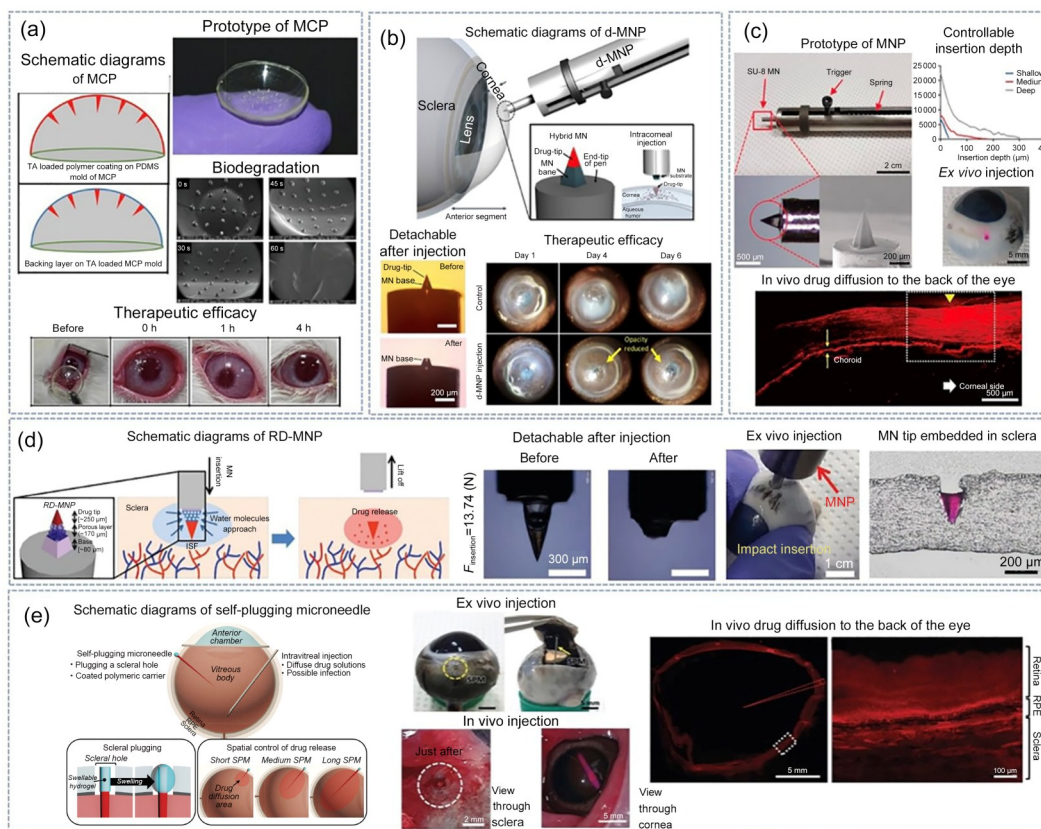


Fig. 9 Microneedle (MN)-based applications for ocular drug delivery. (a) A concave-shaped microneedle corneal patch assuming the semi-spherical structure of the lens (Reprinted from [137], Copyright 2021, with permission from Elsevier B.V.). (b) Hybrid detachable microneedle pen with a biodegradable MN tip for corneal drug delivery (Reprinted from [73], Copyright 2018, with permission from Acta Materialia Inc.). (c) A detachable MN pen with adjustable insertion depths for posterior segment drug delivery (Reprinted from [141], Copyright 2018, with permission from Elsevier B.V.). (d) A rapidly detachable MN pen with a fast-dissolving layer between the drug-loaded tip and base (Reprinted from [142], Copyright 2020, with permission from Wiley-VCH Verlag GmbH & Co., KGaA Weinheim). (e) Self-plugging MN (Reprinted from [143], Copyright 2022, with permission from Wiley-VCH GmbH)

acetone nanosuspensions, which were demonstrated to be biocompatible with ocular tissues using the hen's egg chorioallantoic membrane assay and cytotoxicity test [140]. Thus, these hybrid systems enabled the delivery of drugs to the posterior segment of the eye. Although further investigations are required, these studies offer novel insights into the alleviation of relevant diseases in a therapeutically effective and minimally invasive manner.

Besides the MN array, a single-tip MN can also be used for intrascleral drug delivery. Similar to previous intracorneal strategies, MN pens can be adopted to deliver drugs to the posterior segment. Park et al. [141] developed an MN pen by combining an MN with a customized applicator consisting of an end tip, stopper, trigger, spring, and slot. Ex vivo studies confirmed that the insertion depths of the MNs could be precisely controlled by varying the insertion speed. RB drug-loaded MNs were then administered to beagle eyes in vivo. A strong fluorescent signal was evident along the inner surface of the sclera and choroid from beneath the insertion site to the adjacent area, indicating the

fast diffusion of the model drug to the posterior segment of the eye (Fig. 9c). Lee et al. [142] modified the previously described d-MNP by adding a fast-dissolving layer consisting of a porous blend of PVA/PVP fabricated via freeze-drying and placed between the drug-loaded tip and the base. After optimization, the rapidly detachable microneedle pen demonstrated the almost immediate release of the tip upon contact with the porcine sclera and embedded it at the appropriate depth (Fig. 9d). To resolve needle retraction, Lee et al. [143] developed a self-plugging microneedle (SPM) to perform intraocular drug delivery and simultaneously seal the scleral puncture. Once the entire SPM was completely inserted into the vitreous body, the sclera-plugging component at the bottom of the needle tip would come into contact with the eyeball and swell to plug the scleral hole (Fig. 9e).

Drugs can also be delivered into the space between the sclera and choroid through MN insertion. Hollowed MNs have delivered sulforhodamine B and nanoparticle and microparticle suspensions into the suprachoroidal space of

rabbit, pig, and human eyes [144]. Subsequently, suprachoroidal delivery has become another option for drug delivery to the back of the eye and has been evaluated in animal models of posterior segment diseases and tested in clinical trials [134, 145]. In this application, MN can serve as a tool for initially targeting ocular drug delivery within the eye, and by combining it with other therapies, such as iontophoresis, precisely controlled drug delivery can be easily implemented especially toward the posterior pole [146].

The effectiveness of drug penetration in posterior ocular drug delivery using MN pens has been demonstrated mainly through *in vitro* and *ex vivo* drug delivery experiments. However, further *in vivo* studies are required. Because of the inevitable puncture through the vitreous body during MN implantation, the invasiveness of the operation is currently a major limitation for further application. Thus, determining the optimal insertion route of MN into the target area of the sclera with minimal invasiveness and injuries should be emphasized in further research.

4.3 Gastrointestinal tract

Oral administration of biopharmaceuticals, including peptide and protein drugs, can prevent the pain and risk of infection caused by traditional injections. However, due to barriers in the gastrointestinal (GI) tract, such as an acidic pH environment and the presence of multiple proteases, therapeutic proteins may lose their specific structures and functions, leading to poor permeation efficacy and low bioavailability [147, 148]. Targeted drug delivery systems with specific shielding structures that can deliver the biomolecule precisely to specified sites without any degradation offer a potential solution. Various trials have extensively explored options, such as pH-dependent release [149], micro-robot system [150], micromotors [151], and capsule endoscopy [152, 153]. MNs can pierce the alimentary canal wall without causing gastric perforation and thus potentially improve the treatment for gastric diseases. However, peristalsis of the GI and the flow of chyme pose challenges for the MNs to locate and penetrate the GI mucosa. Therefore, methods of orienting the supplementary component of MNs so that the needles can maintain contact with the tissue surface should be explored in designing drug delivery devices.

Traverso et al. [154] proposed a hollow MN roller encapsulated in a pH-responsive coating that is loaded with insulin for transport into the GI tract. The roller structure ensured that the tips of MNs were always vertical to the GI tract. When the capsule reached the target area, the pH-responsive coating dissolved to expose MNs, and the loaded drug was delivered to the desired location in the GI tract (Fig. 10a). However, the study encountered a low MN fall-off rate and failed to achieve effective targeted drug

delivery. Chen et al. [155] introduced a dynamic omnidirectional adhesive microneedle system (DOAMS) capable of prolonged gastric mucosa fixation, which was inspired by the horny-headed intestinal worm. The smart capsule could either avoid premature exposure of the drug to the harsh pH environment or act as a self-triggered device to deliver a tablet to the stomach. It ejected tablets containing biphasic core-shell-structured MNs into the gastric cavity, thereby inducing appropriate contact with the tissue surface. DOAMS exhibited remarkable adhesion onto GI tissue as a result of both the mechanically interlocking hooks and the material-dependent adhesion of hydrogel MNs (Fig. 10b). Abramson et al. [156] engineered a luminal unfolding MN injector (LUMI) packaged in waterproof enteric capsules that served as a platform to orally deliver therapeutic doses of macromolecule drugs. Upon reaching the small intestine, a compressed spring propels the LUMI out of the capsule regardless of orientation. The LUMI consisted of three degradable arms, each of which bore MNs, which created multiple contact points with the tube-like structures of the small intestine. The rapid unfolding of the support arm created momentum for the piercing of MNs. In the same year, Abramson et al. [157] designed a leopard tortoise-inspired, ingestible, self-orienting millimeter-scale applicator (SOMA), which was able to autonomously adjust its positions to engage with GI tissue. Once the SOMA was in the right position, the pH-triggered spring was released, pushing the single MN into the GI mucosa (Fig. 10c). The capsule, equipped with drug-loaded MNs, can also be driven to the desired target lesions by magnetic force. In 2020, a multilayer MN patch combined with a neodymium permanent magnet capsule was developed [158]. The movements of the magnetically driven capsule were divided into a locomotion state or delivery state according to the relative position between the permanent magnet and the capsule body. By adjusting between the two movements under an external magnetic field, the capsule successfully implemented localized GI drug delivery *ex vivo*.

Most orientation tests and drug delivery experiments of capsuled MNs are still performed *ex vivo*, and *in vivo* animal studies exploring the treatment effect of current devices are lacking. Breakthroughs in follow-up studies should focus on evaluating *in vivo* MN insertion performance, drug release efficiency, and the biosafety of capsule systems. More assessments should be made of the oral administration of the devices or the safety of discharging the nondegradable shell into the GI tract.

4.4 Oral cavity

The oral mucosa is considered a minimally invasive and immunologically rich site that is a potential alternative drug delivery site for topical formulations. The advantages of

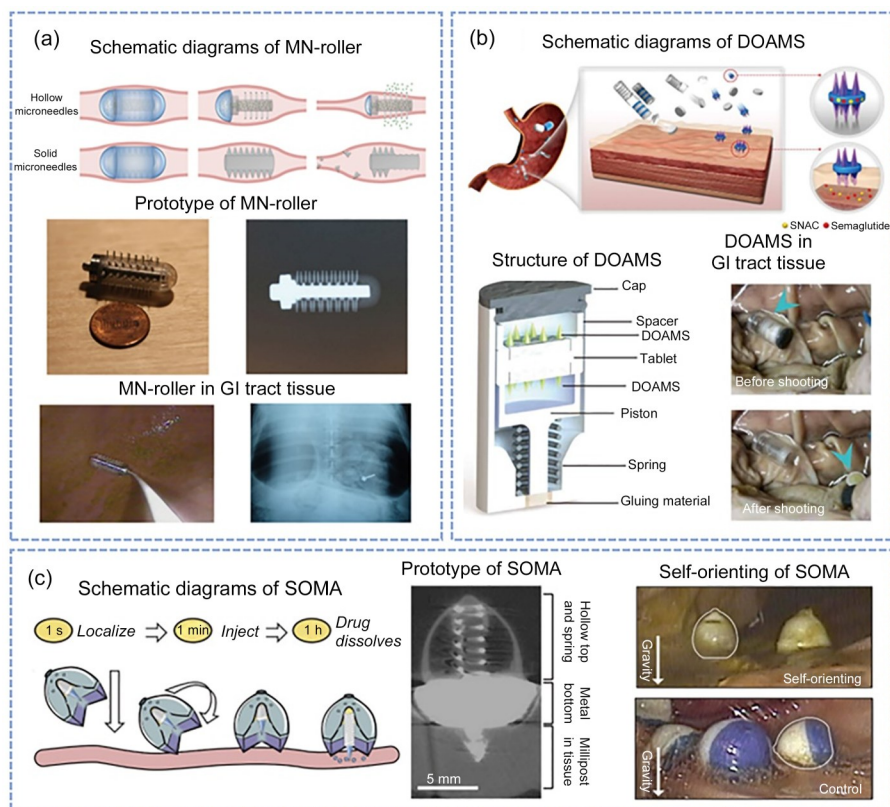


Fig. 10 Microneedle (MN)-based applications for drug delivery into the gastrointestinal tract. (a) A hollow MN roller capsule for drug delivery under a harsh pH environment (Reprinted from [154], Copyright 2014, with permission from Wiley Periodicals, Inc. and the American Pharmacists Association). (b) Dynamic omnidirectional adhesive microneedle system (Reprinted from [155], Copyright 2022, with permission from the authors and exclusive licensee American Association for the Advancement of Science). (c) Self-orienting millimeter-scale applicator (Reprinted from [157], Copyright 2019, with permission from the authors and exclusive licensee American Association for the Advancement of Science)

drug delivery via the transmucosal route include rapid action, reduced first-pass metabolism, and lower drug degradation. MNs enable precise control over drug and vaccine delivery properties, including penetration depth, uniformity, and dosing, making them a strong choice for transmucosal drug delivery via the oral cavity [159, 160]. The first use of oral mucosal drug delivery through MNs was reported in 2014. Researchers used single-row coated MNs to successfully transport drugs to either the inner lip or the dorsal tongue of rabbits. Both experiments showed ideal penetration ability and delivery efficiency with no significant difference, which confirmed that MNs can be ideal tools for drug and vaccine delivery through the oral mucosa [161].

The oral cavity has a moist environment with saliva flux that constantly flushes the oral mucosa, dilutes the drug, and reduces the contact of topical preparations and their bioavailability. This is a phenomenon called “saliva flushing” [162]. Serpe et al. [163] conducted a simulated saliva flow experiment and proved that saliva will wash away a portion of the drug deposited in the oral mucosal tissue using coated MNs, resulting in decreased efficiency in drug administration. For the treatment of dental diseases, such as periodontitis, biodegradable MN patches that can be

inserted into the pocket between the tooth and gingival tissue can help confer a painless and suture-free placement regardless of saliva secretion [164]. Despite the selection of special insertion sites, drug concentration and a multilayer design can also reduce the impact of saliva flushing. Caffarel-Salvador et al. [165] prepared an MN patch with a large amount of drug-loaded buccal macromolecule delivery by directly embedding solid active pharmaceutical ingredients in sorbitol and PVP. Preferential settlement of the drug into the MN tips was achieved by centrifuging the mold at 4000 r/min for 10 min during the molding process to obtain clinically relevant, highly concentrated MNs capable of drug delivery. The deposition of active pharmaceutical ingredients ensures that the medicine can resist the reduced therapeutic effect caused by saliva flushing (Fig. 11a). To achieve efficient and precise drug release, Li et al. [166] prepared composite MNs through a two-step casting process to ensure that the drug was concentrated in the tips. By additionally attaching a mucoadhesive PVA layer and a waterproof ethyl cellulose backing, the MN patch could remain in contact with the lesion for a long time without being eroded by saliva. Cheng et al. [167] fabricated a double-layer composite MN patch to effectively deliver triamcinolone

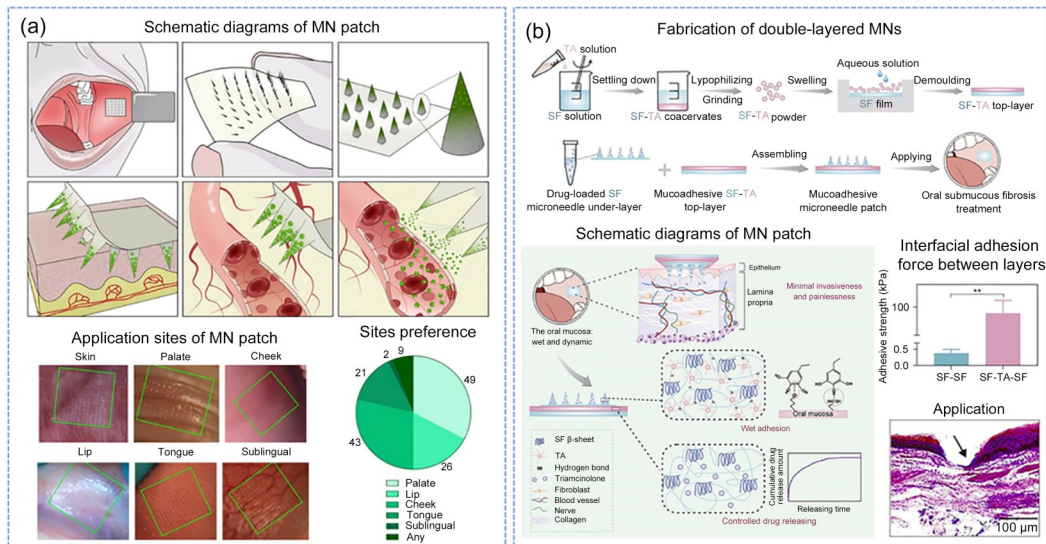


Fig. 11 Microneedle (MN) applications for oral mucosal drug delivery. (a) MN patch fabricated by two-step casting, with the drug deposited on the tips (Reprinted from [165], Copyright 2021, with permission from the authors and exclusive licensee American Association for the Advancement of Science). (b) Double-layered MN patch with enhanced wet adhesion performance (Reprinted from [167], Copyright 2023, with permission from the authors, licensed under CC BY)

to the lesion site for the treatment of oral submucous fibrosis. The mucoadhesive top layer consisted of an adhesive pyrogallol-rich tannic acid/silk fibroin gel film to achieve wet adhesion and a non-adhesive silk fibroin handling film to prevent adhesion to surrounding tissues, which together exhibited an enhanced wet adhesion performance. The experiment also measured the interfacial adhesion force between the two layers (94.54 kPa) to confirm that the MN patch would not delaminate during deployment (Fig. 11b). In addition, the oral cavity is abundant with nerves, which might cause intense pain during injection, resulting in low administration compliance and efficiency [168]. Therefore, strategies to minimize the pain of MNs are crucial. Through clinical trials, Caffarel-Salvador et al. [165] explored the relationship between pain and the choice of administration site when MNs are used for oral mucosa drug delivery. The results revealed that the palates and cheeks have the lowest pain and are most suitable for MN administration. Conversely, the sublingual might be the most painful administration site (Fig. 11a). Further large-scale clinical investigations are imperative to determine the optimal course of treatment.

4.5 Applications to other tissues

4.5.1 Central nervous system

In addition to the abovementioned applications, the uses of MNs have been explored for the central nervous system, including the spinal cord and brain. Han et al. [169] proposed a controlled 3D-exohydrogel hybrid MN array to deliver

3D cultured exosomes derived from mesenchymal stem cells, which has great potential in spinal cord injury therapy (Fig. 12a). Although MNs effectively regulated the immune response and scar formation and promoted spinal cord regeneration, the therapies were quite risky. Implantation may require complicated and potentially dangerous surgical procedures involving the opening of the spine, and any carelessness may cause severe secondary trauma, such as paralysis.

The primary difficulty in brain drug delivery is penetrating the blood-brain barrier (BBB). Current methods for brain drug transportation mainly focus on the nose-to-brain pathway, which brings medicines directly and noninvasively into the brain bypassing the BBB [170]. Considering that MNs can overcome the limitations of systemic delivery and achieve targeted transfection, they have become a promising candidate for brain drug delivery. A heterogenous silk fibroin MN (SMN) patch designed by Wang et al. [171] could circumvent the BBB and release multiple drugs directly to the tumor site for combination drug treatment of glioblastoma. The biocompatible and biodegradable SMN patch could be remotely triggered by NIR to induce rapid drug delivery at a designated stage after implantation, then dissolved slowly over time, allowing the sustained release of multiple drugs at different doses (Fig. 12b). Liu et al. [172] presented a GelMA MN-based platform for the treatment of ischemic stroke and repair of other neurologically diseased tissues. The MNs sustained and controlled the local delivery of adeno-associated virus that expressed human VEGF and achieved homogenous distribution and high transfection efficiency of the load in the ischemic brain.

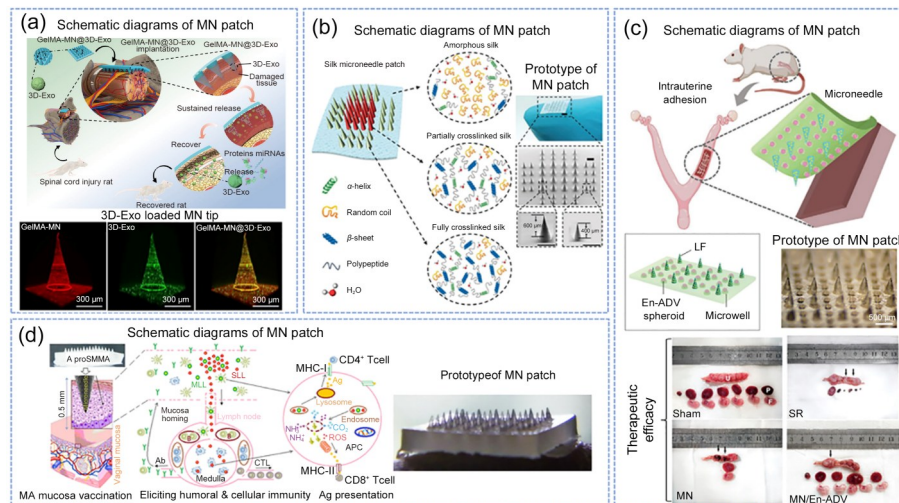


Fig. 12 Microneedle (MN) applications for drug delivery to other tissues. (a) Gelatin methacryloyl MN patch loaded with 3D-exosomes derived from mesenchymal stem cells for the treatment of spinal cord injury (Reprinted from [169], Copyright 2022, with permission from the American Chemical Society). (b) A silk fibroin biodegradable MN patch with a controlled multiple-drug release mechanism for brain hemostasis and treatment of glioblastoma (Reprinted from [171], Copyright 2021, with permission from Wiley-VCH GmbH). (c) A patch for the treatment of intrauterine adhesions, on which MNs loaded with lactoferrin and microwells for the culture of endometrium-derived adventitial cells (En-ADVs) are arranged alternately (Reprinted from [173], Copyright 2022, with permission from Wiley-VCH GmbH). (d) A multifunctional liposome-loaded MN patch for vaginal vaccine delivery (Reprinted from [175], Copyright 2016, with permission from Elsevier B.V.)

Although invasive, these strategies can be applied to other neurological disorders, such as traumatic brain injury or cerebral hemorrhage.

Given the unavoidable requirement of craniotomy during MN patch placement, future clinical conversions of these MN products may encounter substantial challenges because of the associated high surgical risk. Solutions for achieving long-term MN implantation into brain tissue without causing infection or other side effects are worthy of further consideration. Compared with existing noninvasive nose-to-brain drug delivery pathways, further explorations should be conducted in optimizing the drug release efficiency of MNs and enhancing the advantages of long-term drug permeation during MN application to counteract its invasiveness.

4.5.2 Female reproductive system

In the past years, several studies have used MNs for uterine regeneration and intrauterine adhesion (IUA) therapy. Li et al. [173] developed an MN patch combining stem cell-based therapy with the MN tool for in situ intrauterine repair. The flexible MNs were composed of lactoferrin, which conferred high bioactivity, biocompatibility, and antibacterial activity. An array of microwells on MNs enabled the loaded human endometrium-derived adventitial cells (En-ADVs) to form 3D cell spheroids, which exhibited a higher potential for cell proliferation, differentiation, and migration than dissociated cells. The MN patch was designed to better fit the intrauterine surface and achieve stable placement in the uterine tissue by conforming to its shape. The

MN/En-ADV resulted in well-defined myometrial regeneration, angiogenesis, and increased endometrial receptivity, as demonstrated in an Asherman's syndrome rat model (Fig. 12c). Zhang et al. [174] proposed basic fibroblast growth factor (b-FGF) encapsulated in a novel MN patch with arrowhead structures and anisotropic surface adhesion used for treating IUAs. The bioactive N-acryloyl-glycinamide (NAGA) and adhesive poly(ethylene glycol) methacrylate (PEGMA) base materials confer the MNs with anisotropic surface adhesion to adjust to the irregular morphology of the uterus. Manufactured using a multistep micromolding method, the arrowhead structures allowed the MNs to tightly attach to the endometrium. The results of in vivo studies demonstrated that these biocompatible MNs displayed effective inhibition of tissue adhesion and showed better tissue regeneration. Other options for the insertion route of MNs for the treatment of intrauterine lesions include the delivery of patches via the vagina or integration with current gynecological laparoscopic surgery.

Besides the uterus, the vaginal cavity is suitable for the inoculation of mucosal vaccines against sexually transmitted pathogens and is considered a novel site for MN drug delivery. Wang et al. [175] developed a dissolving MN array made of sucrose, PVP, and CMC for stably loaded, protein-based vaccine agents. Two types of multifunctional lipid liposomes (the stealth lipid A-liposome (SLL) and the mannosylated lipid A-liposome (MLL)) loaded with a model antigen and NH_4HCO_3 were fabricated together into the needles to form the proSLL/MLL-constituted MN array (proSMMA). As a vaginal mucosal

vaccine, the administration of proSMMA successfully induced the establishment of humoral and cellular immunity in treated mice (Fig. 12d). Because intravaginal drug delivery has become a novel vaccine delivery method with promising application prospects, further investigations on combining various vaccine delivery methods with MNs should be conducted. However, studies on vaginal drug delivery using

MN technology are scarce. Furthermore, the moist and curved features of the vaginal wall pose a limitation to its applicability as a drug delivery site. To address this challenge, MNs with a flexible configuration resembling endovascular drug delivery systems can be fabricated, while a supporting scaffold can be used to facilitate MN implantation (Table 1).

Table 1 Applications of microneedles (MNs) in different tissues

Tissue	Type	Material	Drug	Specific consideration	Fabrication method	Reference
Tunica adventitia	Dissolving	PLGA50/50 (tips) PLGA90/10 (base and cuff)	Rhodamine B	Cuff shape formed by annealing in a cylinder mold enables better tissue adhesion; fast degradation of MN allows effective drug delivery	Thermal drawing	[118]
	Dissolving, drug-coated	PLGA90/10	Paclitaxel	Curving shape formed by annealing in a cylinder mold enables better adhesion to the target region; drug volume is controlled by the dipping depth during dip coating	Thermal drawing	[119]
	Dissolving, drug-coated	PLGA90/10	Paclitaxel, sirolimus, and sunitinib	Cuff shape formed by annealing in a cylinder mold enables targeted tissue adhesion; dip coating of the drug allows sustained drug delivery	Thermal drawing	[120]
	Dissolving, drug-coated	PLGA80/20 (MNs) PLGA90/10 (mesh)	Sirolimus	Flexible mesh base enables MNs to wrap around vessels to achieve better tissue adhesion	Transfer molding	[75]
	Dissolving	Silk	Sirolimus	Flexible and porous wrap base enables better tissue adhesion of MNs and shows ideal biocompatibility under long-term wrapping; degradation of MNs allows sustained drug delivery	Transfer molding	[74]
Tunica intima	Hollow	Stainless steel (35-gauge)	Dexamethasone	The device has been approved by the Food and Drug Administration for clinical use		[123]
	Drug-coated	UV-curable adhesive 208CTH-F	Paclitaxel	Combining MNs with drug-eluting balloons enables better tissue adhesion and achieves efficient drug delivery	Transfer molding	[124]
	Hydrogel	NAGA (MNs) Gelatin with BP (layer)	Sirolimus	Combining MNs with balloon catheters enables better tissue adhesion; NIR-triggered MN exposure allows controllable and targeted drug delivery	Transfer molding	[125]
Myocardium	Dissolving	PVA	Cardiac stem cells (CSCs)	The porous structure allows the permeation of CSCs through the MNs; the slow dissolution of MNs provides sustained CSC release	Micromolding	[127]

To be continued

Table 1 (continued)

Tissue	Type	Material	Drug	Specific consideration	Fabrication method	Reference
Myocardium	Hydrogel	Crosslinked elastin-like polypeptides (MN tips) Non-crosslinked hyaluronic acid (MN base)	Mesenchymal stromal cell-secreted factor-loaded PLGA nanoparticles	Detachment of MNs after insertion allows close tissue insertion and sustained drug delivery	Multistep casting	[128]
	Hydrogel	PVA	Adeno-associated virus encoding vascular endothelial growth factor gene (AAV-VEGF)	Swellable MNs enable better tissue adhesion and enable the burst release of loaded therapeutic agents into precise regions	Micromolding	[129]
	Hydrogel	Silk fibroin (non-swelling tips) Hyaluronic acid (swelling root)	Biofunctional peptide-fused bioengineered mussel adhesive protein (MAP-BFP)	Swelling hydrogel films coated on MNs enable better tissue adhesion and effective drug delivery	Multistep casting	[130]
	Dissolving	Gelatin	Exosomes containing <i>microRNA-29b</i>	Exosomes are loaded via the soaking method; fast degradation of MNs allows effective drug delivery	Micromolding	[131]
Cornea	Dissolving	PVP-K90 (MNs) PVP-K90/PVA/PEG-400 (back layer)	Cyclosporine A (CsA)	Semi-sphere feature enables better corneal adhesion	Micromolding	[136]
	Drug-coated	Photoresist SU-8	Sunitinib malate	Microneedle pen with a single MN tip and a spring-loaded MN applicator enables impact insertion; dip coating of the drug allows effective drug delivery	Transfer molding	[72]
	Dissolving	PLGA5050 (MN tip) Photoresist SU-8 (MN base)	Polyhexamethylene biguanide (PHMB)	Microneedle pen with a detachable MN tip enables localized insertion; the dissolving capacity of MN allows long-term drug delivery	Transfer molding	[73]
Cornea, sclera	Dissolving	PVP-K90 (MNs) Chitosan/PVA/ PVP-K90 (back layer)	Triamcinolone acetonide (TA)	Concave shape enables better adhesion to the eyeball; the dissolving capacity of MNs allows effective drug delivery	Micromolding	[137]
Sclera	Drug-coated	Photoresist SU-8	Rhodamine B	Loaded spring of the microneedle pen enables depth-controlled impact insertion; dip coating of the drug allows effective drug delivery	Transfer molding	[141]
	Dissolving	PLGA (MN tip) PVP/PVA (porous layer) Photo-curable polymer SU-8 (MN base)	Rhodamine B	The porous PVA/PVP layer of MN allows immediate detachment and insertion of the tip after contact with the sclera; the dissolving capacity of MN enables long-term drug delivery	Transfer molding	[142]
	Drug coated	PLA (needle) PLGA (coating) MeHA (plugging)	Rhodamine B	The plugging component swells after injection to plug the hole and avoid needle retraction; dip coating of the drug allows effective drug delivery	Thermal drawing	[143]

To be continued

Table 1 (continued)

Tissue	Type	Material	Drug	Specific consideration	Fabrication method	Reference
Suprachoroidal space	Hollow	Stainless steel (33-gauge)	Sulprostone, brimonidine	Highly targeted delivery to the supraciliary space	Laser	[144]
GI tract	Hollow	Stainless steel (25-gauge)	Insulin	MN roller with a pH-responsive degradable coating enables targeted MN exposure and insertion	Needles are fitted manually into the central metallic core	[154]
	Hydrogel	Carbopol (shell) PCL (core)	Semaglutide, sodium N-[8(2hydroxybenzoyl) amino] caprylate (SNAC)	Tube-shaped and self-triggered capsule system enables drug delivery in harsh pH environments; core-shell-structured MNs enable sustained drug delivery	Multistep casting	[155]
	Dissolving	PVP	Insulin	Breakable pH-triggered capsule system with a compressed spring enables targeted MN injection under harsh pH environments; the dissolving capacity of MNs enables effective drug delivery	Micromolding and 3D printing	[156]
	Dissolving	PEO/hydroxypropyl methylcellulose	Insulin	Self-orienting capsule system with a pH-triggered spring allows targeted MN injection under harsh pH environments; the dissolving capacity of MNs allows effective drug delivery	Micromolding	[157]
	Dissolving	Gelatin (MN patch) PDMS (layer)	Rhodamine 6G	Magnetic capsule system allows located drug delivery; three-layer MN patches can be sequentially separated to achieve target lesion insertion	Micromolding and 3D printing	[158]
Oral focus	Dissolving	PVP	Human insulin, human growth hormone (hGH)	Drug-concentrated MN tips overcome saliva flushing; degradation of MNs allows effective drug delivery	Two-step casting	[165]
	Dissolving	Hyaluronic acid (MN tips) PVP (base) PVP/ethyl cellulose (backing)	Betamethasone sodium phosphate (BSP)	Waterproof backing layer and drug-concentrated MN tips overcome saliva flushing; degradation of MNs allows effective drug delivery	Two-step casting	[166]
	Hydrogel	Silk fibroin (MN tips) Tannic acid/silk fibroin (top layer)	Triamcinolone	Hydrogel film enables wet adhesion onto the oral mucosa	Multistep casting	[167]
Spinal cord	Hydrogel	GelMA	Three-dimensional cultured mesenchymal stem cells exosomes (MSCs 3D-Exo)	Hydrogel MNs with high biocompatibility and degradability	Micromolding	[169]
Brain	Dissolving	Silk fibroin	Thrombin, temozolomide	Degradation of MNs allows sustained drug release, which can be controlled by adjusting the degree of crosslinking	Micromolding	[171]

To be continued

Table 1 (continued)

Tissue	Type	Material	Drug	Specific consideration	Fabrication method	Reference
Brain	Hydrogel	GelMA	Adeno-associated virus expressing human vascular endothelial growth factor (AAV-VEGF)	Swelling MNs enable better tissue adhesion; degradation of MNs allows effective drug delivery; both the swelling ratio and degradation rate can be controlled by crosslinking durations	Micromolding	[172]
Uterus	Hydrogel	GelMA	Human endometrium-derived adventitial cells (En-ADV)s and lactoferrin	Alternately arranged MNs and cell culture microwells for the delivery of dual therapeutic agents	Micromolding	[173]
	Dissolving	NAGA/PEGMA	Basic fibroblast growth factor (b-FGF)	Arrow-shaped MNs designed for the irregular morphology of the uterus enable close adhesion to the endometrium; the dissolving capacity of MNs allows sustained drug delivery	Multistep casting	[174]
Vagina	Dissolving	Sucrose/PVP/CMC	NH ₄ ⁺ HCO ₃ ⁻ loaded multifunctional liposomes	An MN array is fabricated to fit the vaginal anatomy; the dissolving capacity of MN allows sustained drug delivery	Micromolding	[175]

PLGA: poly(lactic-co-glycolic acid); NAGA: N-acryloylglycinamide; PVA: poly(vinyl alcohol); PVP: polyvinyl pyrrolidone; PEG: polyethylene glycol; MeHA: methacrylated hyaluronic acid; PCL: polycaprolactone; PEO: polyethylene oxide; PDMS: polydimethylsiloxane; GelMA: gelatin methacryloyl; PEGMA: poly(ethylene glycol) methacrylate; CMC: carboxymethylcellulose; UV: ultraviolet

5 Conclusions and future perspectives

MNs have shown tremendous potential, not only in the field of transdermal drug delivery but also in drug administration to many other tissues. This review summarized the current trends in the use of MN-based devices for non-transdermal drug delivery. Specific considerations, including materials, fabrication methods, and design strategies for controlled drug release, were discussed. MN patches with various tip geometries can be fabricated using technologies based on traditional semiconductor technology, such as wet or dry etching and photolithography. Novel additive manufacturing, such as 3D or 4D printing, can also be used to rapidly create diverse shapes at a low cost. Drawing lithography facilitates the development of high-aspect-ratio polymeric MNs without harsh manufacturing conditions. In addition, multistep casting and transfer molding techniques derived from conventional micromolding methods enable the fabrication of applicator devices for facile and standardized MN insertion. By selecting specific hydrogels with a controllable crosslinking rate and flexibly adjusting the assembly strategies of the layered structure, various release mechanisms of loaded drugs can be obtained, including long-term diffusion, triggered release, or responsive release. These features confer MNs with enhanced drug permeability through

various biological barriers. Furthermore, we comprehensively reviewed the applications of MNs for drug delivery to various organs and soft tissues, including vascular, cardiac, ocular, GI, oral, spinal, cerebral, uterine, and vaginal tissues. To achieve close adhesion to the curved structure of blood vessels for vascular drug delivery, flexible and flexional materials should be selected to form a primary cuff base. Methods, such as thermal drawing or transfer molding, which would be convenient for fabricating MNs onto the existing substrate, can be used. When preparing MN patches for MI treatment, biocompatible materials should be used to ensure that the stem cell therapeutic agents remain active. Swellable hydrogels are preferred in achieving secure fixation onto the myocardium. For the manufacturing of MNs for ocular drug delivery, the spherical shape of the eyeball should be considered, such as by fabricating curved patches by micromolding. Another design strategy is to fabricate a detachable single MN tip with an assistant pen structure through transfer molding, which can implement impact insertion with minimal invasiveness and sustained drug release. For MNs designed for GI administration, the devices should be fabricated as capsule systems to withstand harsh pH environments. 3D printing is often used during the fabrication of complex capsule shells, whereas MNs can be simply prepared through micromolding. Moreover,

assistive structures, such as triggers, are needed to enable the devices to attain controllable MN exposure without being disrupted by GI peristalsis. For oral MN drug delivery, a design combining drug-concentrated tips with a waterproof back layer is desirable to bypass saliva flushing and enhance wet adhesion. Multistep casting is a potential fabrication method for achieving oral MN patches with a multi-layered structure. For MNs that deliver therapeutic agents to the nervous system, the main consideration is the selection of applicable polymers for MN fabrication. Biocompatible materials, such as HA and silk fibroin, should be prioritized. The fabrication of MNs for drug delivery to the female reproductive system should consider ideal tissue adhesion capacity. Swellable hydrogel MNs can be further manufactured with arrowhead tips through multistep casting. The specific geometry of MNs may also enable long-term drug release with enhanced permeation efficiency. By designing and manufacturing MN-based devices suitable for the target tissue, close adhesion, ideal penetration, and high drug permeation efficiency can be achieved to outperform traditional drug delivery methods.

MNs integrated with sensors have already been used in the diagnosis and direct monitoring of physiological parameters, medications, and biomarkers [176, 177]. In combination with advanced biosensor technology, intelligent non-transdermal drug delivery devices may enable intuitional surveillance of patients' real-time reactions to drug administration [178, 179]. MN arrays could be fabricated to consist of two sections: the drug release and monitoring sections. For the drug release section, a specific polymer or hydrogel can be selected to achieve programmed drug delivery, whereas the MNs in the monitoring section can function as sensors fabricated using biosensing materials and transmitting electronic and chemical signals. Using the feedback data, the entire MN system can be used to monitor the condition of target tissues and self-regulate the permeation behavior of drugs until the ideal therapeutic effect is achieved. Such devices can accurately determine the patient's drug demand and response to achieve a personalized drug release strategy. Although challenging, these prospective systems can provide more efficient and convenient treatment options and reduce discomfort during the treatment process.

Furthermore, the clinical use and commercialization of MNs are both urgent goals waiting to be achieved. Extensive research has been conducted into skin therapeutic applications, and clinical conversion and primary commercialization of MN devices are already ongoing [180, 181]. However, investigations remain in the early stages for MN-based systems for non-transdermal drug delivery. Systematic clinical trials need to be conducted so that the risks of applying MNs can be evaluated, and corresponding improvements can be provided. As emphasized in this work,

drug delivery strategies to distinct tissues are faced with corresponding dilemmas. The drug delivery route using MNs was originally intended as a minimally invasive method to address the issue of low administration efficiency. However, when applied in non-transdermal settings, the insertion of MNs onto the surface of the target tissue involves significant surgical risks and may result in adverse effects, which contradicts the original applications. This inherent contradiction needs to be further addressed. Therefore, seeking suitable strategies for the implantation of non-transdermal MNs is imperative to minimize surgical injuries and prevent unnecessary tissue damage. Furthermore, another common limitation of non-transdermal MNs is that studies are still primarily conducted on small animals. Thus, the applicability of the therapeutic effects of these MN-based products to humans remains unelucidated. Once the solutions to these key problems are found, further research on human applications, especially clinical trials, can then be initiated. Subsequently, *in vivo* experiments on large animals can be gradually implemented until appropriate clinical applications can be achieved. Designing the structure of MNs to meet patients' individual needs would finally be considered, so that customization of therapeutic interventions may be achieved, especially in using non-transdermal drug delivery through MNs.

Acknowledgements The authors would like to acknowledge financial support from the Beijing Natural Science Foundation (No. L234020), the National Natural Science Foundation of China (Nos. 12472325 and 12272032), and the 111 Project (No. B13003).

Author contributions Conceptualization, XZJ and XFN; writing—original draft, JHX and XYL; writing—review & editing, all authors; supervision, XZJ and XFN.

Declarations

Conflict of interest The authors declare that they have no conflict of interest.

Ethical approval This article does not contain any studies with human or animal subjects performed by any of the authors.

References

1. Prausnitz MR, Langer R (2008) Transdermal drug delivery. *Nat Biotechnol* 26(11):1261–1268. <https://doi.org/10.1038/nbt.1504>
2. Kovacic A, Kopecna M, Vavrova K (2020) Permeation enhancers in transdermal drug delivery: benefits and limitations. *Expert Opin Drug Deliv* 17(2):145–155. <https://doi.org/10.1080/17425247.2020.1713087>
3. Al Hanbali OA, Khan HMS, Sarfraz M et al (2019) Transdermal patches: design and current approaches to painless drug delivery. *Acta Pharm* 69(2):197–215. <https://doi.org/10.2478/acph-2019-0016>

4. Ayala ES, Meuret AE, Ritz T (2009) Treatments for blood-injury-injection phobia: a critical review of current evidence. *J Psychiatr Res* 43(15):1235–1242. <https://doi.org/10.1016/j.jpsychires.2009.04.008>
5. Henry S, McAllister DV, Allen MG et al (1998) Microfabricated microneedles: a novel approach to transdermal drug delivery. *J Pharm Sci* 87(8):922–925. <https://doi.org/10.1021/js980042+>
6. Al-Japairai KAS, Mahmood S, Almurisi SH et al (2020) Current trends in polymer microneedle for transdermal drug delivery. *Int J Pharm* 587:119673. <https://doi.org/10.1016/j.ijpharm.2020.119673>
7. Waghule T, Singhvi G, Dubey SK et al (2019) Microneedles: a smart approach and increasing potential for transdermal drug delivery system. *Biomed Pharmacother* 109:1249–1258. <https://doi.org/10.1016/j.biopha.2018.10.078>
8. Wang RX, Wang JG, Gao HQ et al (2023) Composite double-layer microneedle loaded with traditional Chinese medicine for the treatment of androgenic alopecia. *Med Novel Technol Device* 18:100216. <https://doi.org/10.1016/j.medntd.2023.100216>
9. Hao Y, Li W, Zhou XL et al (2017) Microneedles-based transdermal drug delivery systems: a review. *J Biomed Nanotechnol* 13(12):1581–1597. <https://doi.org/10.1166/jbn.2017.2474>
10. Yadav PR, Dobson LJ, Pattanayek SK et al (2022) Swellable microneedles based transdermal drug delivery: mathematical model development and numerical experiments. *Chem Eng Sci* 247:117005. <https://doi.org/10.1016/j.ces.2021.117005>
11. Wang Y, Liu H, Yang X et al (2023) A responsive hydrogel-based microneedle system for minimally invasive glucose monitoring. *Smart Mater Med* 4:69–77. <https://doi.org/10.1016/j.smaim.2022.07.006>
12. Chen ZJ, He JJ, Qi JP et al (2020) Long-acting microneedles: a progress report of the state-of-the-art techniques. *Drug Discov Today* 25(8):1462–1468. <https://doi.org/10.1016/j.drudis.2020.05.006>
13. Bhatnagar S, Gadeela PR, Thathireddy P et al (2019) Microneedle-based drug delivery: materials of construction. *J Chem Sci* 131:90. <https://doi.org/10.1007/s12039-019-1666-x>
14. Aldawood FK, Andar A, Desai S (2021) A comprehensive review of microneedles: types, materials, processes, characterizations and applications. *Polymers* 13(16):2815. <https://doi.org/10.3390/polym13162815>
15. Li WZ, Huo MR, Zhou JP et al (2010) Super-short solid silicon microneedles for transdermal drug delivery applications. *Int J Pharm* 389(1):122–129. <https://doi.org/10.1016/j.ijpharm.2010.01.024>
16. Kim S, Shetty S, Price D et al (2006) Skin penetration of silicon dioxide microneedle arrays. In: *International Conference of the IEEE Engineering in Medicine and Biology Society*, p.4088–4091. <https://doi.org/10.1109/IEMBS.2006.260142>
17. Gittard SD, Narayan RJ, Jin C et al (2009) Pulsed laser deposition of antimicrobial silver coating on Ormocer[®] microneedles. *Biofabrication* 1(4):041001. <https://doi.org/10.1088/1758-5082/1/4/041001>
18. Choi HJ, Bondy BJ, Yoo DG et al (2013) Stability of whole inactivated influenza virus vaccine during coating onto metal microneedles. *J Contr Release* 166(2):159–171. <https://doi.org/10.1016/j.jconrel.2012.12.002>
19. Shirkhazadeh M (2005) Microneedles coated with porous calcium phosphate ceramics: effective vehicles for transdermal delivery of solid trehalose. *J Mater Sci Mater Med* 16(1):37–45. <https://doi.org/10.1007/s10856-005-6444-2>
20. Wang W, Zhang L, Sun L et al (2018) Biocompatibility and immunotoxicology of the preclinical implantation of a collagen-based artificial dermal regeneration matrix. *Biomed Environ Sci* 31(11):829–842. <https://doi.org/10.3967/bes2018.110>
21. Li ZW, Ruan CS, Niu XF (2023) Collagen-based bioinks for regenerative medicine: fabrication, application and prospective. *Med Novel Technol Device* 17:100211. <https://doi.org/10.1016/j.medntd.2023.100211>
22. Bhadale RS, Londhe VY (2021) A systematic review of carbohydrate-based microneedles: current status and future prospects. *J Mater Sci Mater Med* 32(8):89. <https://doi.org/10.1007/s10856-021-06559-x>
23. Yalcintas EP, Ackerman DS, Korkmaz E et al (2020) Analysis of in vitro cytotoxicity of carbohydrate-based materials used for dissolvable microneedle arrays. *Pharm Res* 37(3):33. <https://doi.org/10.1007/s11095-019-2748-7>
24. Moore LE, Vucen S, Moore AC (2022) Trends in drug- and vaccine-based dissolvable microneedle materials and methods of fabrication. *Eur J Pharm Biopharm* 173:54–72. <https://doi.org/10.1016/j.ejpb.2022.02.013>
25. Moronkeji K, Todd S, Dawidowska I et al (2017) The role of subcutaneous tissue stiffness on microneedle performance in a representative in vitro model of skin. *J Contr Release* 265:102–112. <https://doi.org/10.1016/j.jconrel.2016.11.004>
26. Naves L, Dhand C, Almeida L et al (2017) Poly(lactic-co-glycolic) acid drug delivery systems through transdermal pathway: an overview. *Prog Biomater* 6(1-2):1–11. <https://doi.org/10.1007/s40204-017-0063-0>
27. Grayson ACR, Voskerician G, Lynn A et al (2004) Differential degradation rates in vivo and in vitro of biocompatible poly(lactic acid) and poly(glycolic acid) homo- and co-polymers for a polymeric drug-delivery microchip. *J Biomater Sci Polym Ed* 15(10):1281–1304. <https://doi.org/10.1163/1568562041959991>
28. Turner JG, White LR, Estrela P et al (2021) Hydrogel-forming microneedles: current advancements and future trends. *Macromol Biosci* 21(2):e2000307. <https://doi.org/10.1002/mabi.202000307>
29. Li JY, Mooney DJ (2016) Designing hydrogels for controlled drug delivery. *Nat Rev Mater* 1(12):16071. <https://doi.org/10.1038/natrevmats.2016.71>
30. Huff M (2021) Recent advances in reactive ion etching and applications of high-aspect-ratio microfabrication. *Micromachines* 12(8):991. <https://doi.org/10.3390/mi12080991>
31. O'Mahony C, Sebastian R, Tjulkins F et al (2023) Hollow silicon microneedles, fabricated using combined wet and dry etching techniques, for transdermal delivery and diagnostics. *Int J Pharm* 637:122888. <https://doi.org/10.1016/j.ijpharm.2023.122888>

32. Mamun AA, Zhao F (2022) In-plane Si microneedles: fabrication, characterization, modeling and applications. *Micromachines* 13(5):657. <https://doi.org/10.3390/mi13050657>
33. Rad ZF, Prewett PD, Davies GJ (2021) An overview of microneedle applications, materials, and fabrication methods. *Beilstein J Nanotechnol* 12(1):1034–1046. <https://doi.org/10.3762/bjnano.12.77>
34. Howells O, Blayney GJ, Gualeni B et al (2022) Design, fabrication, and characterisation of a silicon microneedle array for transdermal therapeutic delivery using a single step wet etch process. *Eur J Pharm Biopharm* 171:19–28. <https://doi.org/10.1016/j.ejpb.2021.06.005>
35. Hamzah AA, Abd Aziz N, Yeop Majlis B et al (2012) Optimization of HNA etching parameters to produce high aspect ratio solid silicon microneedles. *J Micromech Microeng* 22(9):95017. <https://doi.org/10.1088/0960-1317/22/9/095017>
36. Berry CA, Smith ZR, Collins SD et al (2020) Dermal ISF collection using a Si microneedle array. In: *IEEE 33rd International Conference on Micro Electro Mechanical Systems*, p.365–368. <https://doi.org/10.1109/MEMS46641.2020.9056394>
37. Li Y, Zhang H, Yang RF et al (2019) Fabrication of sharp silicon hollow microneedles by deep-reactive ion etching towards minimally invasive diagnostics. *Microsyst Nanoeng* 5(1):41. <https://doi.org/10.1038/s41378-019-0077-y>
38. Wang J, Wang H, Lai LY et al (2020) Preparation of microneedle array mold based on MEMS lithography technology. *Micromachines* 12(1):23. <https://doi.org/10.3390/mi12010023>
39. Pradeep Narayanan S, Raghavan S (2016) Solid silicon microneedles for drug delivery applications. *Int J Adv Manuf Tech* 93(1-4):407–422. <https://doi.org/10.1007/s00170-016-9698-6>
40. Roh H, Yoon YJ, Park JS et al (2021) Fabrication of high-density out-of-plane microneedle arrays with various heights and diverse cross-sectional shapes. *Nano-Micro Lett* 14(1):24. <https://doi.org/10.1007/s40820-021-00778-1>
41. Yang QL, Zhong WZ, Xu L et al (2021) Recent progress of 3D-printed microneedles for transdermal drug delivery. *Int J Pharmaceut* 593:120106. <https://doi.org/10.1016/j.ijpharm.2020.120106>
42. Li R, Zhang L, Jiang XB et al (2022) 3D-printed microneedle arrays for drug delivery. *J Contr Release* 350:933–948. <https://doi.org/10.1016/j.jconrel.2022.08.022>
43. Kumar H, Kim K (2020) Stereolithography 3D bioprinting. In: Crook JM (Ed.), *Methods in Molecular Biology*. Humana, New York, USA, p.93–108. https://doi.org/10.1007/978-1-0716-0520-2_6
44. Fei P, Ding H, Duan Y et al (2021) Utility of TPP-manufactured biophysical restrictions to probe multiscale cellular dynamics. *Bio-Des Manuf* 4(4):776–789. <https://doi.org/10.1007/s42242-021-00163-2>
45. Cordeiro AS, Tekko IA, Jomaa MH et al (2020) Two-photon polymerisation 3D printing of microneedle array templates with versatile designs: application in the development of polymeric drug delivery systems. *Pharm Res* 37(9):174. <https://doi.org/10.1007/s11095-020-02887-9>
46. Liao CZ, Anderson W, Antaw F et al (2019) Two-photon nanolithography of tailored hollow three-dimensional microdevices for biosystems. *ACS Omega* 4(1):1401–1409. <https://doi.org/10.1021/acsomega.8b03164>
47. Rad ZF, Nordon RE, Anthony CJ et al (2017) High-fidelity replication of thermoplastic microneedles with open microfluidic channels. *Microsyst Nanoeng* 3(1):17034. <https://doi.org/10.1038/micronano.2017.34>
48. Zhu W, Ma XY, Gou ML et al (2016) 3D printing of functional biomaterials for tissue engineering. *Curr Opin Biotech* 40:103–112. <https://doi.org/10.1016/j.copbio.2016.03.014>
49. Willems NGA, Morsink MAJ, Veerman D et al (2022) From oral formulations to drug-eluting implants: using 3D and 4D printing to develop drug delivery systems and personalized medicine. *Bio-Des Manuf* 5(1):85–106. <https://doi.org/10.1007/s42242-021-00157-0>
50. Miao SD, Cui HT, Nowicki M et al (2018) Photolithographic-stereolithographic-tandem fabrication of 4D smart scaffolds for improved stem cell cardiomyogenic differentiation. *Biofabrication* 10(3):035007. <https://doi.org/10.1088/1758-5090/aabe0b>
51. Cui HT, Liu CY, Esworthy T et al (2020) 4D physiologically adaptable cardiac patch: a 4-month in vivo study for the treatment of myocardial infarction. *Sci Adv* 6(26):eabb5067. <https://doi.org/10.1126/sciadv.abb5067>
52. Lee J, Park SH, Seo IH et al (2015) Rapid and repeatable fabrication of high A/R silk fibroin microneedles using thermally-drawn micromolds. *Eur J Pharm Biopharm* 94:11–19. <https://doi.org/10.1016/j.ejpb.2015.04.024>
53. Choi CK, Lee KJ, Youn YN et al (2013) Spatially discrete thermal drawing of biodegradable microneedles for vascular drug delivery. *Eur J Pharm Biopharm* 83(2):224–233. <https://doi.org/10.1016/j.ejpb.2012.10.020>
54. Lee K, Jung H (2012) Drawing lithography for microneedles: a review of fundamentals and biomedical applications. *Biomaterials* 33(30):7309–7326. <https://doi.org/10.1016/j.biomaterials.2012.06.065>
55. Lee K, Park SH, Lee J et al (2019) Three-step thermal drawing for rapid prototyping of highly customizable microneedles for vascular tissue insertion. *Pharmaceutics* 11(3):100. <https://doi.org/10.3390/pharmaceutics11030100>
56. Onesto V, Di Natale C, Profeta M et al (2020) Engineered PLGA-PVP/VA based formulations to produce electro-drawn fast biodegradable microneedles for labile biomolecule delivery. *Prog Biomater* 9(4):203–217. <https://doi.org/10.1007/s40204-020-00143-2>
57. Ruggiero F, Vecchione R, Bhowmick S et al (2018) Electro-drawn polymer microneedle arrays with controlled shape and dimension. *Sens Actuat B Chem* 255:1553–1560. <https://doi.org/10.1016/j.snb.2017.08.165>
58. Kim JD, Kim M, Yang H et al (2013) Droplet-born air blowing: novel dissolving microneedle fabrication. *J Contr Release* 170(3):430–436. <https://doi.org/10.1016/j.jconrel.2013.05.026>
59. Chen ZP, Ye R, Yang JB et al (2019) Rapidly fabricated microneedle arrays using magnetorheological drawing lithography for transdermal drug delivery. *ACS Biomater Sci Eng* 5(10):5506–5513. <https://doi.org/10.1021/acsbomaterials.9b00919>
60. Chen ZP, Ren L, Li JY et al (2018) Rapid fabrication of

- microneedles using magnetorheological drawing lithography. *Acta Biomater* 65:283–291.
<https://doi.org/10.1016/j.actbio.2017.10.030>
61. Chen ZP, Lin YY, Lee W et al (2018) Additive manufacturing of honeybee-inspired microneedle for easy skin insertion and difficult removal. *ACS Appl Mater Interfaces* 10(35):29338–29346.
<https://doi.org/10.1021/acsami.8b09563>
 62. Ahrbekoh FN, Salimi L, Saghati S et al (2022) Application of microneedle patches for drug delivery; doorstep to novel therapies. *J Tissue Eng* 13:20417314221085390.
<https://doi.org/10.1177/20417314221085390>
 63. Wang QL, Zhu DD, Chen Y et al (2016) A fabrication method of microneedle molds with controlled microstructures. *Mater Sci Eng C* 65:135–142.
<https://doi.org/10.1016/j.msec.2016.03.097>
 64. Silvestre SL, Araujo D, Marques AC et al (2020) Microneedle arrays of polyhydroxyalkanoate by laser-based micromolding technique. *ACS Appl Bio Mater* 3(9):5856–5864.
<https://doi.org/10.1021/acsabm.0c00570>
 65. Anbazhagan G, Suseela SB, Sankararajan R (2023) Design, analysis and fabrication of solid polymer microneedle patch using CO₂ laser and polymer molding. *Drug Deliv Transl Res* 13(6):1813–1827.
<https://doi.org/10.1007/s13346-023-01296-w>
 66. Lin YH, Lee IC, Hsu WC et al (2016) Rapid fabrication method of a microneedle mold with controllable needle height and width. *Biomed Microdev* 18(5):85.
<https://doi.org/10.1007/s10544-016-0113-8>
 67. Hatsuzawa T, Kurosaka M (2018) A cell culture device equipped with a micro-needle electrode array fabricated using backside exposure mold and resin casting. *Biomed Microdev* 20(3):58.
<https://doi.org/10.1007/s10544-018-0303-7>
 68. Wang ZJ, Fu RX, Han X et al (2022) Shrinking fabrication of a glucose-responsive glucagon microneedle patch. *Adv Sci* 9(28):e2203274.
<https://doi.org/10.1002/advs.202203274>
 69. Zhang Y, Wang DF, Gao MY et al (2018) Separable microneedles for near-infrared light-triggered transdermal delivery of metformin in diabetic rats. *Acs Biomater Sci Eng* 4(8):2879–2888.
<https://doi.org/10.1021/acsbiomaterials.8b00642>
 70. Chen MC, Lai KY, Ling MH et al (2018) Enhancing immunogenicity of antigens through sustained intradermal delivery using chitosan microneedles with a patch-dissolvable design. *Acta Biomater* 65:66–75.
<https://doi.org/10.1016/j.actbio.2017.11.004>
 71. Chu LY, Prausnitz MR (2011) Separable arrowhead microneedles. *J Contr Release* 149(3):242–249.
<https://doi.org/10.1016/j.jconrel.2010.10.033>
 72. Song HB, Lee KJ, Seo IH et al (2015) Impact insertion of transfer-molded microneedle for localized and minimally invasive ocular drug delivery. *J Contr Release* 209:272–279.
<https://doi.org/10.1016/j.jconrel.2015.04.041>
 73. Lee K, Song HB, Cho W et al (2018) Intracorneal injection of a detachable hybrid microneedle for sustained drug delivery. *Acta Biomater* 80:48–57.
<https://doi.org/10.1016/j.actbio.2018.09.039>
 74. Lee J, Jang EH, Kim JH et al (2021) Highly flexible and porous silk fibroin microneedle wraps for perivascular drug delivery. *J Contr Release* 340:125–135.
<https://doi.org/10.1016/j.jconrel.2021.10.024>
 75. Lee J, Kim DH, Lee KJ et al (2017) Transfer-molded wrappable microneedle meshes for perivascular drug delivery. *J Contr Release* 268:237–246.
<https://doi.org/10.1016/j.jconrel.2017.10.007>
 76. Yang L, Yang Y, Chen HZ et al (2022) Polymeric microneedle-mediated sustained release systems: design strategies and promising applications for drug delivery. *Asian J Pharm Sci* 17(1):70–86.
<https://doi.org/10.1016/j.ajps.2021.07.002>
 77. Oleksy M, Dynarowicz K, Aebischer D (2023) Advances in biodegradable polymers and biomaterials for medical applications—a review. *Molecules* 28(17):6213.
<https://doi.org/10.3390/molecules28176213>
 78. Mbituyimana B, Ma GR, Shi ZJ et al (2022) Polymer-based microneedle composites for enhanced non-transdermal drug delivery. *Appl Mater Today* 29:101659.
<https://doi.org/10.1016/j.apmt.2022.101659>
 79. Yang FH, Wang JX, Li XY et al (2022) Electrospinning of a sandwich-structured membrane with sustained release capability and long-term anti-inflammatory effects for dental pulp regeneration. *Bio-Des Manuf* 5(2):305–317.
<https://doi.org/10.1007/s42242-021-00152-5>
 80. Ma GJ, Wu CW (2017) Microneedle, bio-microneedle and bio-inspired microneedle: a review. *J Contr Release* 251:11–23.
<https://doi.org/10.1016/j.jconrel.2017.02.011>
 81. Zhang XX, Wang FY, Yu YR et al (2019) Bio-inspired clamping microneedle arrays from flexible ferrofluid-configured moldings. *Sci Bull* 64(15):1110–1117.
<https://doi.org/10.1016/j.scib.2019.06.016>
 82. Zhang XX, Chen GP, Sun LY et al (2021) Claw-inspired microneedle patches with liquid metal encapsulation for accelerating incisional wound healing. *Chem Eng J* 406:126741.
<https://doi.org/10.1016/j.cej.2020.126741>
 83. Lu YW, Ren TC, Zhang H et al (2022) A honeybee stinger-inspired self-interlocking microneedle patch and its application in myocardial infarction treatment. *Acta Biomater* 153:386–398.
<https://doi.org/10.1016/j.actbio.2022.09.015>
 84. Liu TQ, Sun YF, Jiang GH et al (2023) Porcupine-inspired microneedles coupled with an adhesive back patching as dressing for accelerating diabetic wound healing. *Acta Biomater* 160:32–44.
<https://doi.org/10.1016/j.actbio.2023.01.059>
 85. Yang SY, O’Cearbhaill ED, Sisk GC et al (2013) A bio-inspired swellable microneedle adhesive for mechanical interlocking with tissue. *Nat Commun* 4(1):1702.
<https://doi.org/10.1038/ncomms2715>
 86. Seong KY, Seo MS, Hwang DY et al (2017) A self-adherent, bullet-shaped microneedle patch for controlled transdermal delivery of insulin. *J Contr Release* 265:48–56.
<https://doi.org/10.1016/j.jconrel.2017.03.041>
 87. Jeon EY, Lee J, Kim BJ et al (2019) Bio-inspired swellable hydrogel-forming double-layered adhesive microneedle protein patch for regenerative internal/external surgical closure. *Biomaterials* 222:119439.
<https://doi.org/10.1016/j.biomaterials.2019.119439>
 88. Uppu DSSM, Turvey ME, Sharif ARM et al (2020) Temporal

- release of a three-component protein subunit vaccine from polymer multilayers. *J Contr Release* 317:130–141. <https://doi.org/10.1016/j.jconrel.2019.11.022>
89. Jung CR, Lahiji SF, Kim Y et al (2020) Rapidly separable micropillar integrated dissolving microneedles. *Pharmaceutics* 12(6):581. <https://doi.org/10.3390/pharmaceutics12060581>
90. Li W, Terry RN, Tang J et al (2019) Rapidly separable microneedle patch for the sustained release of a contraceptive. *Nat Biomed Eng* 3(3):220–229. <https://doi.org/10.1038/s41551-018-0337-4>
91. Lee Y, Li W, Tang J et al (2021) Immediate detachment of microneedles by interfacial fracture for sustained delivery of a contraceptive hormone in the skin. *J Contr Release* 337:676–685. <https://doi.org/10.1016/j.jconrel.2021.08.012>
92. Ning TQ, Yang FH, Chen DL et al (2022) Synergistically detachable microneedle dressing for programmed treatment of chronic wounds. *Adv Healthc Mater* 11(11):e2102180. <https://doi.org/10.1002/adhm.202102180>
93. Yang FH, Niu XF, Gu XN et al (2019) Biodegradable magnesium-incorporated poly(L-lactic acid) microspheres for manipulation of drug release and alleviation of inflammatory response. *ACS Appl Mater Interfaces* 11(26):23546–23557. <https://doi.org/10.1021/acsami.9b03766>
94. Ke CJ, Lin YJ, Hu YC et al (2012) Multidrug release based on microneedle arrays filled with pH-responsive PLGA hollow microspheres. *Biomaterials* 33(20):5156–5165. <https://doi.org/10.1016/j.biomaterials.2012.03.056>
95. Vora LK, Donnelly RF, Larraneta E et al (2017) Novel bilayer dissolving microneedle arrays with concentrated PLGA nanoparticles for targeted intradermal delivery: proof of concept. *J Contr Release* 265:93–101. <https://doi.org/10.1016/j.jconrel.2017.10.005>
96. Yang FH, Xu CP, Zhang W et al (2023) Biodegradable magnesium incorporated microspheres enable immunomodulation and spatiotemporal drug release for the treatment of osteonecrosis of the femoral head. *Compos Part B Eng* 250:110430. <https://doi.org/10.1016/j.compositesb.2022.110430>
97. Mazzara JM, Ochyl LJ, Hong JKY et al (2019) Self-healing encapsulation and controlled release of vaccine antigens from PLGA microparticles delivered by microneedle patches. *Bioeng Transl Med* 4(1):116–128. <https://doi.org/10.1002/btm2.10103>
98. Tran KTM, Gavitt TD, Farrell NJ et al (2021) Transdermal microneedles for the programmable burst release of multiple vaccine payloads. *Nat Biomed Eng* 5(9):998–1007. <https://doi.org/10.1038/s41551-020-00650-4>
99. Li W, Chen JY, Terry RN et al (2022) Core-shell microneedle patch for six-month controlled-release contraceptive delivery. *J Contr Release* 347:489–499. <https://doi.org/10.1016/j.jconrel.2022.04.051>
100. Makvandi P, Jamaledin R, Chen GJ et al (2021) Stimuli-responsive transdermal microneedle patches. *Mater Today* 47:206–222. <https://doi.org/10.1016/j.mattod.2021.03.012>
101. Ding HT, Tan P, Fu SQ et al (2022) Preparation and application of pH-responsive drug delivery systems. *J Contr Release* 348:206–238. <https://doi.org/10.1016/j.jconrel.2022.05.056>
102. Percival SL, McCarty S, Hunt JA et al (2014) The effects of pH on wound healing, biofilms, and antimicrobial efficacy. *Wound Repair Regen* 22(2):174–186. <https://doi.org/10.1111/wrr.12125>
103. Mo R, Zhang H, Xu Y et al (2023) Transdermal drug delivery via microneedles to mediate wound microenvironment. *Adv Drug Deliv Rev* 195:114753. <https://doi.org/10.1016/j.addr.2023.114753>
104. Lei XL, Cheng K, Li Y et al (2023) The eradication of biofilm for therapy of bacterial infected chronic wound based on pH-responsive micelle of antimicrobial peptide derived biodegradable microneedle patch. *Chem Eng J* 462:142222. <https://doi.org/10.1016/j.cej.2023.142222>
105. Yan GQ, Wang J, Hu LF et al (2017) Stepwise targeted drug delivery to liver cancer cells for enhanced therapeutic efficacy by galactose-grafted, ultra-pH-sensitive micelles. *Acta Biomater* 51:363–373. <https://doi.org/10.1016/j.actbio.2017.01.031>
106. Duong HTT, Yin Y, Thambi T et al (2018) Smart vaccine delivery based on microneedle arrays decorated with ultra-pH-responsive copolymers for cancer immunotherapy. *Biomaterials* 185:13–24. <https://doi.org/10.1016/j.biomaterials.2018.09.008>
107. Podual K, Doyle FJ, Peppas NA (2000) Glucose-sensitivity of glucose oxidase-containing cationic copolymer hydrogels having poly(ethylene glycol) grafts. *J Contr Release* 67(1):9–17. [https://doi.org/10.1016/S0168-3659\(00\)00195-4](https://doi.org/10.1016/S0168-3659(00)00195-4)
108. Chen W, Tian R, Xu C et al (2017) Microneedle-array patches loaded with dual mineralized protein/peptide particles for type 2 diabetes therapy. *Nat Commun* 8(1):1777. <https://doi.org/10.1038/s41467-017-01764-1>
109. Yu JC, Zhang YQ, Ye YQ et al (2015) Microneedle-array patches loaded with hypoxia-sensitive vesicles provide fast glucose-responsive insulin delivery. *Proc Natl Acad Sci USA* 112(27):8260–8265. <https://doi.org/10.1073/pnas.1505405112>
110. Hu XL, Yu JC, Qian CG et al (2017) H₂O₂-responsive vesicles integrated with transcutaneous patches for glucose-mediated insulin delivery. *ACS Nano* 11(1):613–620. <https://doi.org/10.1021/acs.nano.6b06892>
111. Yu JC, Wang JQ, Zhang YQ et al (2020) Glucose-responsive insulin patch for the regulation of blood glucose in mice and minipigs. *Nat Biomed Eng* 4(5):499–506. <https://doi.org/10.1038/s41551-019-0508-y>
112. Castellano JM, Narula J, Castillo J et al (2014) Promoting cardiovascular health worldwide: strategies, challenges, and opportunities. *Rev Esp Cardiol* 67(9):724–730. <https://doi.org/10.1016/j.rec.2014.01.023>
113. Li L, Wang L, Liu SS et al (2019) Association between coronary atherosclerotic plaque composition and cardiovascular disease risk. *Biomed Environ Sci* 32(2):75–86. <https://doi.org/10.3967/bes2019.012>
114. Raval AJ, Parikh JK, Desai MA (2023) Perivascular patch using biodegradable polymers: investigation of mechanical and drug elution characteristics. *J Mech Behav Biomed Mater* 142:105853. <https://doi.org/10.1016/j.jmbbm.2023.105853>
115. Kim JH, Jang EH, Ryu JY et al (2023) Sirolimus-embedded silk microneedle wrap to prevent neointimal hyperplasia in vein graft model. *Int J Mol Sci* 24(4):3306.

- <https://doi.org/10.3390/ijms24043306>
116. Filova E, Parizek M, Olsovská J et al (2011) Perivascular sirolimus-delivery system. *Int J Pharm* 404(1-2):94–101. <https://doi.org/10.1016/j.ijpharm.2010.11.005>
 117. Mylonaki I, Allemann E, Saucy F et al (2017) Perivascular medical devices and drug delivery systems: making the right choices. *Biomaterials* 128:56–68. <https://doi.org/10.1016/j.biomaterials.2017.02.028>
 118. Choi CK, Kim JB, Jang EH et al (2012) Curved biodegradable microneedles for vascular drug delivery. *Small* 8(16):2483–2488. <https://doi.org/10.1002/sml.201200441>
 119. Lee KJ, Park SH, Lee JY et al (2014) Perivascular biodegradable microneedle cuff for reduction of neointima formation after vascular injury. *J Contr Release* 192:174–181. <https://doi.org/10.1016/j.jconrel.2014.07.007>
 120. Kim DH, Jang EH, Lee KJ et al (2017) A biodegradable microneedle cuff for comparison of drug effects through perivascular delivery to balloon-injured arteries. *Polymers* 9(2):56. <https://doi.org/10.3390/polym9020056>
 121. Tzafiriri AR, Edelman ER (2016) Endovascular drug delivery and drug elution systems: first principles. *Interv Cardiol Clin* 5(3):307–320. <https://doi.org/10.1016/j.iccl.2016.02.007>
 122. Lee KJ, Lee SG, Jang I et al (2018) Linear micro-patterned drug eluting balloon (LMDEB) for enhanced endovascular drug delivery. *Sci Rep* 8(1):3666. <https://doi.org/10.1038/s41598-018-21649-7>
 123. Owens CD, Gasper WJ, Walker JP et al (2014) Safety and feasibility of adjunctive dexamethasone infusion into the adventitia of the femoropopliteal artery following endovascular revascularization. *J Vasc Surg* 59(4):1016–1024. <https://doi.org/10.1016/j.jvs.2013.10.051>
 124. Lee KJ, Lee JY, Lee SG et al (2020) Microneedle drug eluting balloon for enhanced drug delivery to vascular tissue. *J Contr Release* 321:174–183. <https://doi.org/10.1016/j.jconrel.2020.02.012>
 125. Zhang XX, Cheng Y, Liu R et al (2022) Globefish-inspired balloon catheter with intelligent microneedle coating for endovascular drug delivery. *Adv Sci* 9(34):e2204497. <https://doi.org/10.1002/advs.202204497>
 126. Cheng W, Law PK (2017) Conceptual design and procedure for an autonomous intramyocardial injection catheter. *Cell Transplant* 26(5):735–751. <https://doi.org/10.3727/096368916X694256>
 127. Tang JN, Wang JQ, Huang K et al (2018) Cardiac cell-integrated microneedle patch for treating myocardial infarction. *Sci Adv* 4(11):eaat9365. <https://doi.org/10.1126/sciadv.aat9365>
 128. Hu SQ, Zhu DS, Li ZH et al (2022) Detachable microneedle patches deliver mesenchymal stromal cell factor-loaded nanoparticles for cardiac repair. *ACS Nano* 16(10):15935–15945. <https://doi.org/10.1021/acsnano.2c03060>
 129. Shi HP, Xue T, Yang Y et al (2020) Microneedle-mediated gene delivery for the treatment of ischemic myocardial disease. *Sci Adv* 6(25):eaaz3621. <https://doi.org/10.1126/sciadv.aaz3621>
 130. Lim S, Park TY, Jeon EY et al (2021) Double-layered adhesive microneedle bandage based on biofunctionalized mussel protein for cardiac tissue regeneration. *Biomaterials* 278:121171. <https://doi.org/10.1016/j.biomaterials.2021.121171>
 131. Yuan JQ, Yang H, Liu CX et al (2023) Microneedle patch loaded with exosomes containing microRNA-29b prevents cardiac fibrosis after myocardial infarction. *Adv Healthc Mater* 12(13):e2202959. <https://doi.org/10.1002/adhm.202202959>
 132. Bachu RD, Chowdhury P, Al-Saedi ZHF et al (2018) Ocular drug delivery barriers—role of nanocarriers in the treatment of anterior segment ocular diseases. *Pharmaceutics* 10(1):28. <https://doi.org/10.3390/pharmaceutics10010028>
 133. Falavarjani KG, Nguyen QD (2013) Adverse events and complications associated with intravitreal injection of anti-VEGF agents: a review of literature. *Eye* 27(7):787–794. <https://doi.org/10.1038/eye.2013.107>
 134. Huang D, Chen YS, Rupenthal ID (2018) Overcoming ocular drug delivery barriers through the use of physical forces. *Adv Drug Deliv Rev* 126:96–112. <https://doi.org/10.1016/j.addr.2017.09.008>
 135. Long LY, Ji D, Hu C et al (2023) Microneedles for in situ tissue regeneration. *Mater Today Bio* 19:100579. <https://doi.org/10.1016/j.mtbio.2023.100579>
 136. Datta D, Roy G, Garg P et al (2022) Ocular delivery of cyclosporine A using dissolvable microneedle contact lens. *J Drug Deliv Sci Tec* 70:103211. <https://doi.org/10.1016/j.jddst.2022.103211>
 137. Roy G, Garg P, Venuganti VVK (2022) Microneedle scleral patch for minimally invasive delivery of triamcinolone to the posterior segment of eye. *Int J Pharm* 612:121305. <https://doi.org/10.1016/j.ijpharm.2021.121305>
 138. Than A, Liu CH, Chang H et al (2018) Self-implantable double-layered micro-drug-reservoirs for efficient and controlled ocular drug delivery. *Nat Commun* 9(1):4433. <https://doi.org/10.1038/s41467-018-06981-w>
 139. Wu Y, Vora LK, Wang YJ et al (2021) Long-acting nanoparticle-loaded bilayer microneedles for protein delivery to the posterior segment of the eye. *Eur J Pharm Biopharm* 165:306–318. <https://doi.org/10.1016/j.ejpb.2021.05.022>
 140. Wu Y, Vora LK, Mishra D et al (2022) Nanosuspension-loaded dissolving bilayer microneedles for hydrophobic drug delivery to the posterior segment of the eye. *Biomater Adv* 137:212767. <https://doi.org/10.1016/j.bioadv.2022.212767>
 141. Park SH, Jo DH, Cho CS et al (2018) Depthwise-controlled scleral insertion of microneedles for drug delivery to the back of the eye. *Eur J Pharm Biopharm* 133:31–41. <https://doi.org/10.1016/j.ejpb.2018.09.021>
 142. Lee Y, Park S, Kim SI et al (2020) Rapidly detachable microneedles using porous water-soluble layer for ocular drug delivery. *Adv Mater Technol* 5(5):10. <https://doi.org/10.1002/admt.201901145>
 143. Lee K, Park S, Jo DH et al (2022) Self-plugging microneedle (SPM) for intravitreal drug delivery. *Adv Healthc Mater* 11(12):e2102599. <https://doi.org/10.1002/adhm.202102599>
 144. Patel SR, Lin ASP, Edelhauser HF et al (2011) Suprachoroidal drug delivery to the back of the eye using hollow microneedles. *Pharm Res* 28(1):166–176. <https://doi.org/10.1007/s11095-010-0271-y>
 145. Kim YC, Edelhauser HF, Prausnitz MR (2014) Targeted delivery of antiglaucoma drugs to the supraciliary space using microneedles.

- Invest Ophthalmol Vis Sci 55(11):7387–7397.
<https://doi.org/10.1167/iovs.14-14651>
146. Jung JH, Chiang B, Grossniklaus HE et al (2018) Ocular drug delivery targeted by iontophoresis in the suprachoroidal space using a microneedle. *J Contr Release* 277:14–22.
<https://doi.org/10.1016/j.jconrel.2018.03.001>
 147. Smart AL, Gaisford S, Basit AW (2014) Oral peptide and protein delivery: intestinal obstacles and commercial prospects. *Expert Opin Drug Del* 11(8):1323–1335.
<https://doi.org/10.1517/17425247.2014.917077>
 148. Liu C, Kou YQ, Zhang X et al (2018) Strategies and industrial perspectives to improve oral absorption of biological macromolecules. *Expert Opin Drug Deliv* 15(3):223–233.
<https://doi.org/10.1080/17425247.2017.1395853>
 149. Liu F, Moreno P, Basit AW (2010) A novel double-coating approach for improved pH-triggered delivery to the ileo-colonic region of the gastrointestinal tract. *Eur J Pharm Biopharm* 74(2):311–315.
<https://doi.org/10.1016/j.ejpb.2009.11.008>
 150. Nelson BJ, Kaliakatsos IK, Abbott JJ (2010) Microrobots for minimally invasive medicine. *Annu Rev Biomed Eng* 12(1):55–85.
<https://doi.org/10.1146/annurev-bioeng-010510-103409>
 151. Li JX, Thamphiwatana S, Liu WJ et al (2016) Enteric micromotor can selectively position and spontaneously propel in the gastrointestinal tract. *ACS Nano* 10(10):9536–9542.
<https://doi.org/10.1021/acsnano.6b04795>
 152. Mapara SS, Patravale VB (2017) Medical capsule robots: a renaissance for diagnostics, drug delivery and surgical treatment. *J Contr Release* 261:337–351.
<https://doi.org/10.1016/j.jconrel.2017.07.005>
 153. Munoz F, Alici G, Li WH (2014) A review of drug delivery systems for capsule endoscopy. *Adv Drug Deliv Rev* 71:77–85.
<https://doi.org/10.1016/j.addr.2013.12.007>
 154. Traverso G, Schoellhammer CM, Schroeder A et al (2015) Microneedles for drug delivery via the gastrointestinal tract. *J Pharm Sci* 104(2):362–367.
<https://doi.org/10.1002/jps.24182>
 155. Chen W, Wainer J, Ryoo SW et al (2022) Dynamic omnidirectional adhesive microneedle system for oral macromolecular drug delivery. *Sci Adv* 8(1):eabk1792.
<https://doi.org/10.1126/sciadv.abk1792>
 156. Abramson A, Caffarel-Salvador E, Soares V et al (2019) A luminal unfolding microneedle injector for oral delivery of macromolecules. *Nat Med* 25(10):1512–1518.
<https://doi.org/10.1038/s41591-019-0598-9>
 157. Abramson A, Caffarel-Salvador E, Khang M et al (2019) An ingestible self-orienting system for oral delivery of macromolecules. *Science* 363(6427):611–615.
<https://doi.org/10.1126/science.aau2277>
 158. Lee J, Lee H, Kwon SH et al (2020) Active delivery of multilayer drug-loaded microneedle patches using magnetically driven capsule. *Med Eng Phys* 85:87–96.
<https://doi.org/10.1016/j.medengphy.2020.09.012>
 159. Creighton RL, Woodrow KA (2019) Microneedle-mediated vaccine delivery to the oral mucosa. *Adv Healthc Mater* 8(4):e1801180.
<https://doi.org/10.1002/adhm.201801180>
 160. Wang YQ, Sheng AA, Jiang XR et al (2023) Multidrug dissolvable microneedle patch for the treatment of recurrent oral ulcer. *Bio-Des Manuf* 6(3):255–267.
<https://doi.org/10.1007/s42242-022-00221-3>
 161. Ma YZ, Tao WQ, Krebs SJ et al (2014) Vaccine delivery to the oral cavity using coated microneedles induces systemic and mucosal immunity. *Pharm Res* 31(9):2393–2403.
<https://doi.org/10.1007/s11095-014-1335-1>
 162. An H, Gu Z, Zhou LP et al (2022) Janus mucosal dressing with a tough and adhesive hydrogel based on synergistic effects of gelatin, polydopamine, and nano-clay. *Acta Biomater* 149:126–138.
<https://doi.org/10.1016/j.actbio.2022.07.016>
 163. Serpe L, Jain A, de Macedo CG et al (2016) Influence of salivary washout on drug delivery to the oral cavity using coated microneedles: an in vitro evaluation. *Eur J Pharm Sci* 93:215–223.
<https://doi.org/10.1016/j.ejps.2016.08.023>
 164. Zhang XX, Hasani-Sadrabadi MM, Zarubova J et al (2022) Immunomodulatory microneedle patch for periodontal tissue regeneration. *Matter* 5(2):666–682.
<https://doi.org/10.1016/j.matt.2021.11.017>
 165. Caffarel-Salvador E, Kim S, Soares V et al (2021) A microneedle platform for buccal macromolecule delivery. *Sci Adv* 7(4):eabe2620.
<https://doi.org/10.1126/sciadv.abe2620>
 166. Li XJ, Li Y, Meng Y et al (2022) Composite dissolvable microneedle patch for therapy of oral mucosal diseases. *Biomater Adv* 139:213001.
<https://doi.org/10.1016/j.bioadv.2022.213001>
 167. Cheng X, Yang YQ, Liao ZW et al (2023) Drug-loaded mucoadhesive microneedle patch for the treatment of oral submucous fibrosis. *Front Bioeng Biotechnol* 11:1251583.
<https://doi.org/10.3389/fbioe.2023.1251583>
 168. Chung MK, Wang S, Oh SL et al (2021) Acute and chronic pain from facial skin and oral mucosa: unique neurobiology and challenging treatment. *Int J Mol Sci* 22(11):5810.
<https://doi.org/10.3390/ijms22115810>
 169. Han M, Yang HR, Lu XD et al (2022) Three-dimensional-cultured MSC-derived exosome-hydrogel hybrid microneedle array patch for spinal cord repair. *Nano Lett* 22(15):6391–6401.
<https://doi.org/10.1021/acs.nanolett.2c02259>
 170. Sasaki K, Fukakusa S, Torikai Y et al (2023) Effective nose-to-brain drug delivery using a combination system targeting the olfactory region in monkeys. *J Contr Release* 359:384–399.
<https://doi.org/10.1016/j.jconrel.2023.06.005>
 171. Wang ZJ, Yang ZP, Jiang JJ et al (2022) Silk microneedle patch capable of on-demand multidrug delivery to the brain for glioblastoma treatment. *Adv Mater* 34(1):e2106606.
<https://doi.org/10.1002/adma.202106606>
 172. Liu Y, Long LY, Zhang FJ et al (2021) Microneedle-mediated vascular endothelial growth factor delivery promotes angiogenesis and functional recovery after stroke. *J Contr Release* 338:610–622.
<https://doi.org/10.1016/j.jconrel.2021.08.057>
 173. Li SY, Li YF, Yu F et al (2022) Human endometrium-derived adventitial cell spheroid-loaded antimicrobial microneedles for uterine regeneration. *Small* 18(31):e2201225.
<https://doi.org/10.1002/sml.202201225>
 174. Zhang XX, Chen GP, Wang YT et al (2022) Arrowhead

- composite microneedle patches with anisotropic surface adhesion for preventing intrauterine adhesions. *Adv Sci* 9(12):e2104883. <https://doi.org/10.1002/advs.202104883>
175. Wang N, Zhen YY, Jin YG et al (2017) Combining different types of multifunctional liposomes loaded with ammonium bicarbonate to fabricate microneedle arrays as a vaginal mucosal vaccine adjuvant-dual delivery system (VADDS). *J Contr Release* 246:12–29. <https://doi.org/10.1016/j.jconrel.2016.12.009>
176. Ma SW, Li JQ, Pei LX et al (2023) Microneedle-based interstitial fluid extraction for drug analysis: advances, challenges, and prospects. *J Pharm Anal* 13(2):111–126. <https://doi.org/10.1016/j.jpha.2022.12.004>
177. Huang XH, Liang BM, Zheng ST et al (2023) Microarrow sensor array with enhanced skin adhesion for transdermal continuous monitoring of glucose and reactive oxygen species. *Bio-Des Manuf* 7(1):14–30. <https://doi.org/10.1007/s42242-023-00246-2>
178. Wang Y, Xu HR, Dong ZZ et al (2022) Micro/nano biomedical devices for point-of-care diagnosis of infectious respiratory diseases. *Med Novel Technol Device* 14:100116. <https://doi.org/10.1016/j.medntd.2022.100116>
179. Liu SY, Jia ZZ, Yang FH et al (2023) Flexible transient bioelectronic system enables multifunctional active-controlled drug delivery. *Adv Funct Mater* 33(13):2215034. <https://doi.org/10.1002/adfm.202215034>
180. Bhatnagar S, Dave K, Venuganti VVK (2017) Microneedles in the clinic. *J Contr Release* 260:164–182. <https://doi.org/10.1016/j.jconrel.2017.05.029>
181. Lee KJ, Jeong SS, Roh DH et al (2020) A practical guide to the development of microneedle systems—in clinical trials or on the market. *Int J Pharmaceut* 573:118778. <https://doi.org/10.1016/j.ijpharm.2019.118778>